Journal of Structural Geology 168 (2023) 104823

Contents lists available at ScienceDirect

Journal of Structural Geology

journal homepage: www.elsevier.com/locate/jsg

Deciphering western Mediterranean kinematics using metamorphic porphyroblasts from the Alpujárride Complex (Betic Cordillera)

Alejandro Ruiz-Fuentes [a,*], Domingo G.A.M. Aerden [a,b]

[a] Departamento de Geodinámica, Universidad de Granada, Av. Fuentenueva, 18071, Granada, Spain
[b] Instituto Andaluz de Ciencias de la Tierra, CSIC/Universidad de Granada, Av. de las Palmeras 4, 18100, Armilla, Granada, Spain

ARTICLE INFO

Keywords:
Alpujárride complex
Betic cordillera
Alpine orogeny
Foliation intersection axes
X-ray computed tomography

ABSTRACT

3D microstructural analysis of porphyroblast inclusion trails using X-ray Computed Tomography is integrated with analysis of field structures to unravel the Alpine deformation history of the Alpujárride Complex, which constitutes the partially submerged metamorphic core of the Gibraltar Arc. Prograde metamorphism in the complex has been traditionally linked to a 'D_1' event witnessed by inclusion trails in garnet porphyroblasts. Orientation data for these microstructures reveal three age groups with differently oriented axes of inclusion-trail curvature (known as FIA). The successive development of FIAs trending WNW-ESE, ENE-WSW and NNW-SSE is shown and correlated with the Paleogene-Neogene relative plate-motion paths of Africa, Iberia and the Alborán Domain as known from paleomagnetic data. During the late-metamorphic evolution of the Alpujárride Complex, after garnet growth had ceased, two steeply dipping crenulation cleavages and associated folds with roughly suborthogonal N–S and E-W trends developed, in addition to two subhorizontal ones. Inclusion trails are also found to exhibit a general preference for subvertical and subhorizontal orientations, suggesting a protracted orogenic evolution characterized by multiple stress permutations causing alternations of crustal shortening and gravitational collapse.

1. Introduction

In the Alpujárride Complex of the Betic Cordillera, a succession of at least three tectonic foliations and associated fold sets has been recognized but no consensus has been reached on their tectonic significance (extension, compression, transpression, etc.) and kinematics (see review in e.g. Williams and Platt, 2017; Jabaloy-Sánchez et al., 2019a). These structures are predated by one or several foliations that are only preserved as inclusion trails within garnet porphyroblasts. The latter grew during prograde metamorphism, whereas the main external fabrics formed during decompression. This study focuses on the geometry and preferred orientations of these relic microstructures using oriented thin sections and X-ray computed microtomography (XCT) in 60 samples that span about 200 km distance in E-W direction. This microstructural work is integrated with conventional analysis of structural relationships in outcrop along various transects.

The principle difficulty for interpreting the tectonic significance of relic foliations has traditionally been that their original orientation was uncertain. In recent decades, however, remarkably consistent orientations of inclusion trails found in numerous mountain belts suggest that they preserve the original orientations in which they formed due to a general lack of porphyroblast rotation (e.g. Fyson, 1980; Bell et al., 1992; Hayward, 1992; Aerden, 1995, 1998, 2004; Bell and Forde, 1995; Bell and Welch, 2002; Stallard and Hickey, 2001; Bell et al., 2003; Ham and Bell, 2004; Sayab, 2005; Cihan et al., 2006; Sanislav, 2010; Sanislav and Bell, 2011; Shah et al., 2011; Skrzypek et al., 2011; Bell and Sapkota, 2012; Abu Sharib and Sanislav, 2013; Aerden et al., 2010, 2013, 2021, 2022; Sayab et al., 2016). Inclusion trail data in these studies have consequently allowed extending tectonic reconstructions further back in time and in more detail. Of particular interest are the orientations of so called Foliation Intersection- or Inflexion-Axes (Bell et al., 1995), abbreviated as FIA (equivalent to relative porphyroblast-matrix rotation axes) as they are thought to form normal to the direction of tectonic transport or crustal shortening. Aerden et al. (2022) recently presented a collection of ca. 350 FIA data from the Betic-Rif orogen and showed that they cluster in three sets with distinctive trends (WNW-ESE, NE-SW, and NNW-SSE). Relative timing criteria and Sm–Nd garnet dating supported the sequential formation of the three FIA sets, from the Late Eocene to the Early Miocene, oriented normal to (changing) relative plate-motion vectors between Africa, Iberia and the Alborán Domain. Most of Aerden

* Corresponding author.
E-mail addresses: aruizf@ugr.es (A. Ruiz-Fuentes), aerden@ugr.es (D.G.A.M. Aerden).

https://doi.org/10.1016/j.jsg.2023.104823
Received 7 July 2022; Received in revised form 7 February 2023; Accepted 8 February 2023
Available online 9 February 2023

et al.'s data, however, were collected in the Nevado-Filábride and Sebtide complexes with only 47 individual FIAs coming from the Alpujárride Complex, despite its much larger total outcrop area compared to the other two complexes. In this paper, we present 647 new individual plus 25 average FIAs for the Alpujárride Complex and document their relationships with polyphase structures and fabrics recognizable in the field. This evidence confirms the existence of three FIA sets in the Betic-Rif orogen and supports their relationship with orogen dynamics and the Tertiary paleogeographic evolution of the Western Mediterranean region.

2. Geological setting

2.1. The Betic Cordillera

The Betic Cordillera (Fig. 1) of southern Spain is situated at the western termination of the Mediterranean Alpine system and constitutes the northern branch of the Gibraltar Arc. Its 'Internal Zones' comprise a stack of metamorphic complexes arranged, from bottom to top, as the Nevado-Filábride, Alpujárride and Maláguide complexes. The first is generally considered part of subducted and exhumed South-Iberian crust (Platt et al., 2006; Gómez-Pugnaire et al., 2012; Rodríguez-Cañero et al., 2018), whereas the Alpujárride and Maláguide complexes jointly constitute the so called 'Alborán Domain' which constitutes the core of the Gibraltar Arc and crops out also in the Rif mountains of northern Morocco. The equivalent units of the Alpujárride and Maláguide complexes are called Sebtide complex and Ghomaride complex there. The Alborán domain is derived from a continental fragment known as AlKaPeCa (Bouillin, 1986) or Mesomediterranean Microplate (Guerrera et al., 1993) originally situated east or south-east of Iberia (see review in Guerrera et al., 2021). Westward drift of the Alborán Domain, independent of continuous N–S to NW-SE-changing Iberia-Africa convergence, led to its eventual collision with the South Iberian paleomargin and the development of an external fold-and-thrust belt in Mesozoic and Cenozoic sedimentary rocks of shelf and basin environments corresponding to the present External Zones and Flysch Units (or Campo de Gibraltar Complex), respectively. Cover sediments of the Alborán Domain appear at the front of the Internal Zones as several tectonic slices known as the Frontal Units (or Dorsale Calcaire). These are overthrusted by the Alpujárride-Maláguide stack, but also partially backthrusted onto these complexes (Jabaloy-Sánchez et al., 2019b).

Pre-Alpine structures in the Paleozoic basements of the three complexes are only well preserved in the low-grade to non-metamorphic Maláguide Complex (e.g. Foucault and Paquet, 1971; Balanyá, 1991; Cuevas et al., 2001; Martín-Algarra et al., 2009; Ruiz-Fuentes et al., 2022). In the Alpujárride and Nevado-Filábride complexes, their recognition is complicated by intense Alpine deformation and metamorphism, but nevertheless evidenced by geochronological and petrological data (e.g. Puga and Díaz de Federico, 1976; Sánchez-Navas et al., 2012, 2014, 2017; Acosta-Vigil et al., 2014; Massonne, 2014; Sanz de Galdeano and Ruiz Cruz, 2016).

The Maláguide Complex is only affected by Alpine metamorphism in its lower part, which reached sub-greenschist facies conditions (Nieto et al., 1994; Ruiz Cruz et al., 2005). The Alpujárride Complex underwent high-pressure/low-temperature (HP/LT) metamorphism in the Eocene (Platt et al., 2005; Bessière et al., 2022) followed by progressive heating during the Oligocene and exhumation in the Miocene (Aguado et al., 1990; Crespo-Blanc et al., 1994; Sosson et al., 1998; Sánchez-Rodríguez and Gebauer, 2000; Esteban et al., 2004; Massonne, 2014). Exhumation of the complex was synchronous with HP metamorphism in the Nevado-Filábride Complex (López Sánchez-Vizcaíno et al., 2001; Platt et al., 2006; Kirchner et al., 2016), which was exhumed in the late Miocene (Johnson et al., 1997). Recent geochronological and petrological evidence, however, indicates that the Nevado-Filábrides may have experienced an earlier HP metamorphic event in the Eocene, synchronous with that of the Alpujárride Complex (Augier et al., 2005; Li and Massonne, 2018; Porkoláb et al., 2022; Aerden et al., 2022).

2.2. Alpujárride Complex

The Alpujárride Complex has been traditionally subdivided in a large number of nappe units defined and named in restricted study areas (e.g. Los Reales nappe (Tubía, 1988), Sayalonga unit (Aldaya et al., 1979), Murtas nappe (Aldaya, 1969), La Plata nappe (García-Dueñas and Navarro-Vilá, 1976), etc.). Attempts to regionally correlate these units resulted in partially discrepant proposals (see Sanz de Galdeano and López-Garrido, 2003 for a review). In the Central and eastern Betics, Azañón et al. (1994) distinguished five units called, from bottom to top,

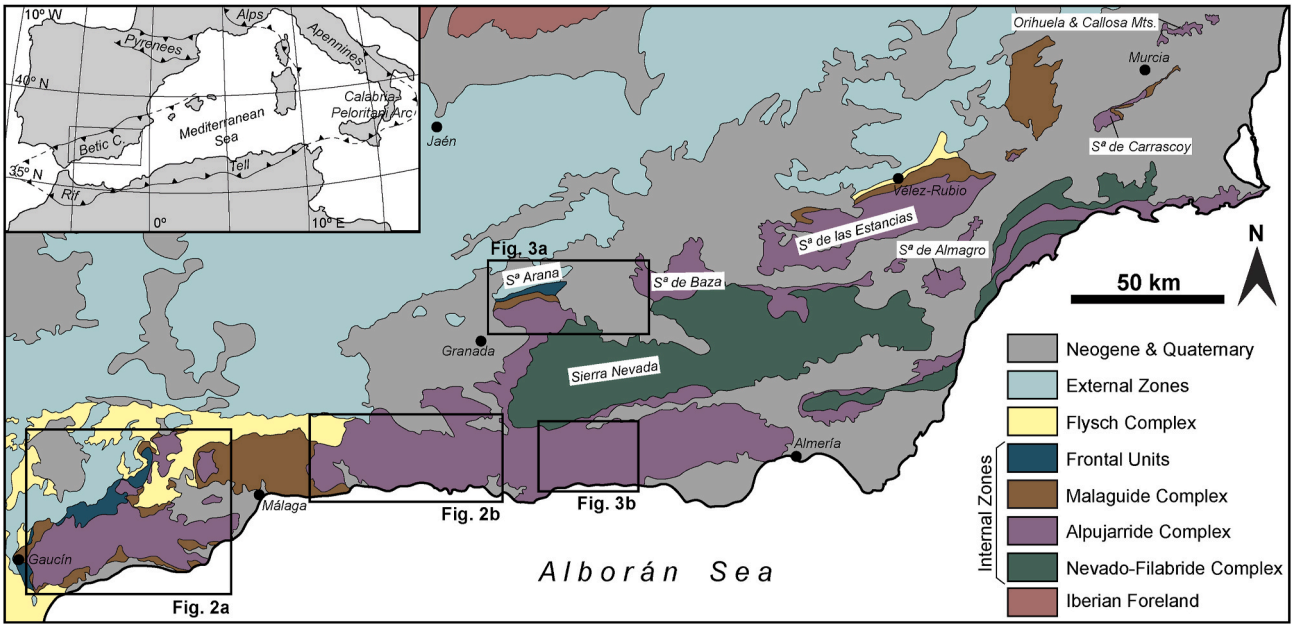

Fig. 1. Geological map of the Internal Zones of the Betic Cordillera, which as the more detailed maps of Figs. 2 and 3 are based on IGME MAGNA 1/50 000 map series.

the Lújar-, Escalate-, Herradura-, Salobreña- and Adra units. Tubía et al. (1992), Sanz de Galdeano and López-Garrido (2003) and Martín-Algarra et al. (2004) proposed three main units, identified as the Lower-, Intermediate- and Upper Units. The latter subdivision is followed in this paper.

The Lower Alpujárride units are composed of Permo-Triassic phyllites and marbles that preserve relics of blueschist-facies metamorphism dated late-Eocene (Azañón and Crespo-Blanc, 2000; Bessière et al., 2022). The Intermediate and Upper units include a portion of Paleozoic basement composed of high-to medium grade migmatites, gneisses and graphite schists overlain by Permo-Triassic light-colored schists and quartzites, phyllites and marbles. In the Western Betics, the Intermediate unit hosts rare eclogite lenses with Jurassic protolith ages (Tubía and Gil-Ibarguchi, 1991; Sánchez-Rodríguez and Gebauer, 2000), whereas the Upper unit (Los Reales nappe) contains a several kilometer thick peridotite slab (Ronda peridotites) at the base of the crustal sequence.

In the Montes de Málaga and Fuengirola areas, the boundary between the Upper Alpujárride units and the Maláguide complex has proven difficult to identify because of similar lithologies and metamorphic grades on both sides. In the Montes de Málaga, an extra 'Benamocarra unit' has been defined with transitional characteristics (e.g. Estévez González and Chamón Cobos, 1978; Aldaya et al., 1979; Elorza and García-Dueñas, 1981). Tubía and Navarro-Vilá (1984) and Tubía (1988) placed the contact at the base of a level of brownish schists containing post-kinematic andalusite and garnet porphyroblasts.

Most structural research in the Alpujárride Complex considers four main deformation phases (D_1-D_4), the first of which corresponds to relics of a HP/LT foliation (S_1) preserved within garnet porphyroblasts and microlithons of the main S_2 regional cleavage (e.g. Azañón and Goffé, 1997; Booth-Rea et al., 2002). The latter is associated with small-scale tight-to isoclinal F_2 folds, except for a possible km-scale structure interpreted in the Sierra de Lujar (Simancas, 2018). In general, however, regional-scale folds have been classified as D_3 structures associated with S_3 crenulation cleavage. They mostly have N- to NW-vergence except in a zone close to the boundary with the External Zones, where an opposite vergence is observed as discussed later. The above succession of ductile structures and fabrics are cut by a series of low-angle detachment faults and shear bands (D_4) with top-to-the-North movement.

D_1 is generally attributed to approximately N–S directed Africa-Eurasia convergence, subduction and crustal shortening in the Eocene to Oligocene, but its precise kinematics (polarity of subduction) has remained uncertain. D_2 has been variably interpreted in terms of extensional exhumation along a low-angle crustal shear zone (Azañón et al., 1997; Balanyá et al., 1997; Azañón and Crespo-Blanc, 2000; Alonso-Chaves and Orozco, 2007; Williams and Platt, 2017, 2018; Simancas, 2018), or transpressional exhumation along a sinistral NE-trending steep shear zone (Tubía et al., 1992; Rossetti et al., 2005). D_3 structures have been alternatively attributed to top-to-the-N/NE crustal extension (Orozco et al., 1998, 2004; Platt, 1998) or thrusting (Cuevas, 1991; Tubía et al., 1992; Simancas and Campos, 1993; Balanyá et al., 1993, 1997, 1998; Azañón et al., 1997; Azañón and Crespo-Blanc, 2000; Simancas, 2018). No agreement exists either on the extensional or thrust character of late D_4 faults (Cuevas et al., 1986; Cuevas, 1991; Simancas and Campos, 1993; Crespo-Blanc et al., 1994; Azañón and Crespo-Blanc, 2000; Simancas, 2018).

3. Structural relationships in outcrop

Orientation data for crenulation-cleavages collected throughout the Alpujárride Complex (Figs. 2 and 3) display a bimodal distribution of steep and shallow dips, which reflects the existence of at least two different age sets exhibiting overprinting relationships in outcrop (Figs. 4–6). In order to avoid confusion and maintain the traditional denomination of crenulation cleavage in the Alpujaride Complex as "S_3", we will further refer to both sets as S_{3V} (steep to subvertical dips, ~60-90°) and S_{3H} (gentle to subhorizontal dips, ~ 0-30°), but note that we interpret a different timing for them. Studied lineations are mainly crenulation lineations, which are usually parallel to intersection and mineral lineations when found in nearby outcrops.

3.1. Jubrique area

In the Jubrique area (Fig. 2a), S_2 is strongly overprinted or fully transposed by a gently west-dipping S_{3H} (Fig. 4a, b, 4c, 7 and 8) associated with synkinematic andalusite porphyroblasts. S_2 generally dips slightly steeper NW to WSW, but locally in opposite (E) direction, especially in the lower part of the schists and quartzites and in the underlying gneisses. S_{3H} reaches its maximum intensity in the middle part of the schist-quartzite succession. Fold- and crenulation axes have NNE-SSW to NNW-SSE trends, but a younger set of E-W-trending kink-like folds was identified in the upper part of the succession.

3.2. Fuengirola area

In the Fuengirola area (south-east of the Sierra Alpujata peridotites; Fig. 2a) S_2 is variably overprinted by either an S_{3V} or S_{3H} (Figs. 4, 5 and 7). South of Sierra Alpujata, S_{3H} is well developed and associated with gently E-dipping shear planes and tight to isoclinal F_{3H} folds with E-W trends. Andalusite porphyroblasts grew synchronous with this foliation and postdate an earlier sillimanite-bearing schistosity (S_2). South of Benalmádena, S_{3H} is more widely spaced and associated with relatively open folds (Fig. 4d).

Between Mijas and Fuengirola (Fig. 2a), two principle sets of S_{3V} and S_{3H} crenulation cleavages were found although their relative timing could not be determined in this area. The first strikes NNW-SSE associated with (Fig. 5a and b) ENE-vergent folds. An additional weaker set of E-W trending folds is also present, which become increasingly important in the Torrox and Almuñécar areas further east (see sections 3.3 and 3.4). In the Contraviesa area, overprinting relationships between E-W and N–S folds (see section 3.6) suggest a later timing of the first. Between La Cala de Mijas and Fuengirola and near Benalmádena, S_{3V} is weaker although F_{3V} folds with NNW-SSE trends are still abundant. From there moving westward, the intensity of S_{3V} diminishes further until, near the eastern boundary of the Sierra Alpujata peridotites, it disappears completely.

3.3. Torrox area

The Torrox area (Fig. 2b) is characterized by a pervasive S_{3H} transposing S_2 (Fig. 4e) in the lower part of the micaschists above the Torrox orthogneiss body. In higher levels, S_{3H} is weaker or absent but F_{3H} folds are locally still prominent. A large number of orientation data for folds and lineations collected by Alonso-Chaves and Orozco (2012) complemented with our own data (Fig. 7) indicate a broadly bimodal trend distribution with a strong E-W maximum and a more dispersed NNW-SSE maximum. Note that fold axes and lineations measured in the Fuengirola area (Fig. 7), although less numerous, exhibit a similar bimodal distribution (section 3.2).

3.4. Almuñécar area

In the Almuñécar area (Fig. 2b), S_{3H} is generally less intense as in the Torrox area but still locally transposes S_2. F_{3H} folds (Fig. 4f) have ENE-WSW to E-W trends and inconsistent vergences. An L_3 lineation is visible in outcrop parallel to fold axes. In the southernmost part of the area, between La Herradura and Salobreña, a steeply dipping widely spaced crenulation cleavage (S_{3V}) with ENE-WSW strike and northward vergence was observed to overprint S_{3H} (Fig. 5c and d).

3.5. Tocón de Quéntar – Sierra de Baza area

In the Tocón de Quéntar area (Fig. 3a), micaschist outcrops are

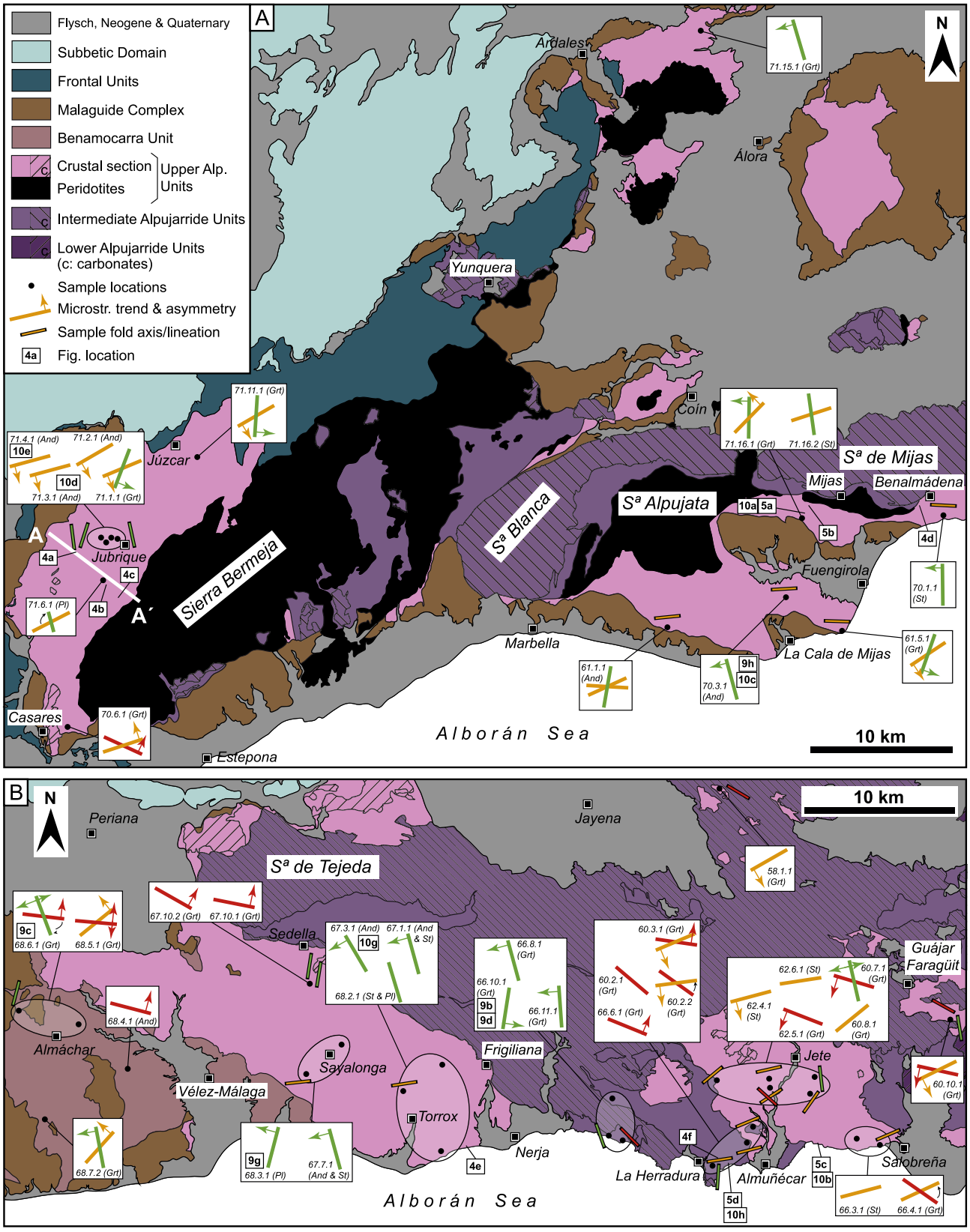

Fig. 2. Geological maps of the Jubrique-Fuengirola (A) and Torrox-Almuñécar (B) areas showing the location of cross sections, outcrop and microstructural images (Figure numbers in small boxes), average microstructural trends indicated with red, orange and green bars corresponding to the three trend ranges defined in Fig. 11, and tectonic transport directions (thin arrows) deduced from inclusion-trail asymmetries. (For interpretation of the references to color in this figure legend, the reader is referred to the Web version of this article.)

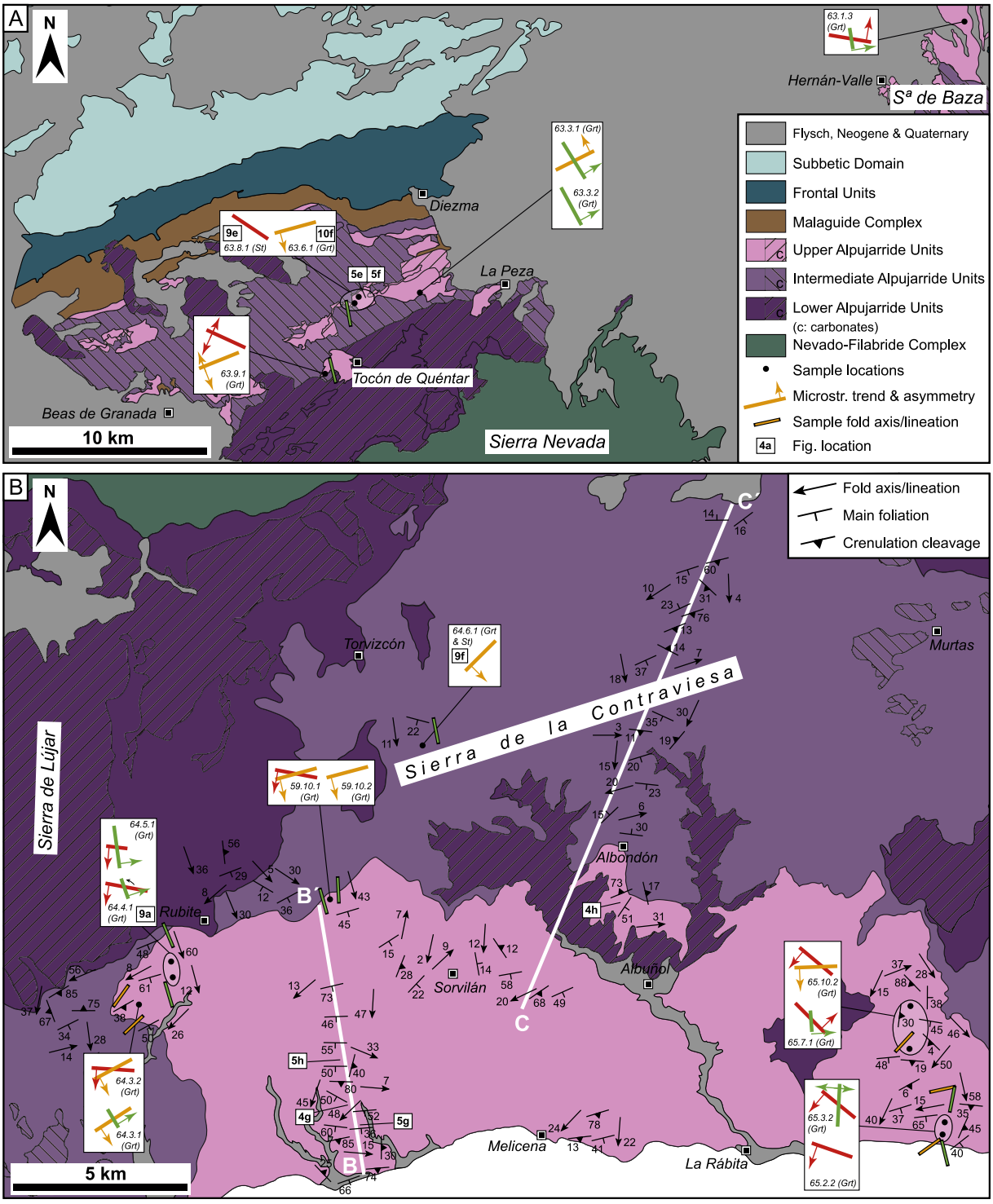

Fig. 3. Geological maps of the Tocón de Quéntar (A) and Contraviesa (B) areas showing the location of cross sections, outcrop and microstructural images (Figure numbers in small boxes), average microstructural trends indicated with red, orange and green bars corresponding to the three trend ranges defined in Fig. 11, and the directions of tectonic transport (thin arrows) deduced from inclusion-trail asymmetries. Map 'A' is partially based on Sanz de Galdeano et al. (1995). (For interpretation of the references to color in this figure legend, the reader is referred to the Web version of this article.)

scarce and correspond to small weathered klippe located on top of carbonate rocks by means of low angle faults probably related to the D_4 low-angle faults and shear bands in the Contraviesa area. The main foliation is overprinted by a spaced S_{3V} crenulation cleavage associated with ENE-WSW- to NE-SW trending folds (Fig. 5e and f, 7). Interestingly, the vergence of these folds is southward (Fig. 5e), opposite to that observed in the Contraviesa area. Orientation data for pre-D_3 folds and lineations suggest two sets of structures with NNW-SSE versus NW-SE to WNW-ESE trends.

3.6. Contraviesa area

In the Contraviesa area (Fig. 3b), S_2 dips moderately to steeply south (Fig. 7) and is overprinted with variable intensity by WSW-ENE striking

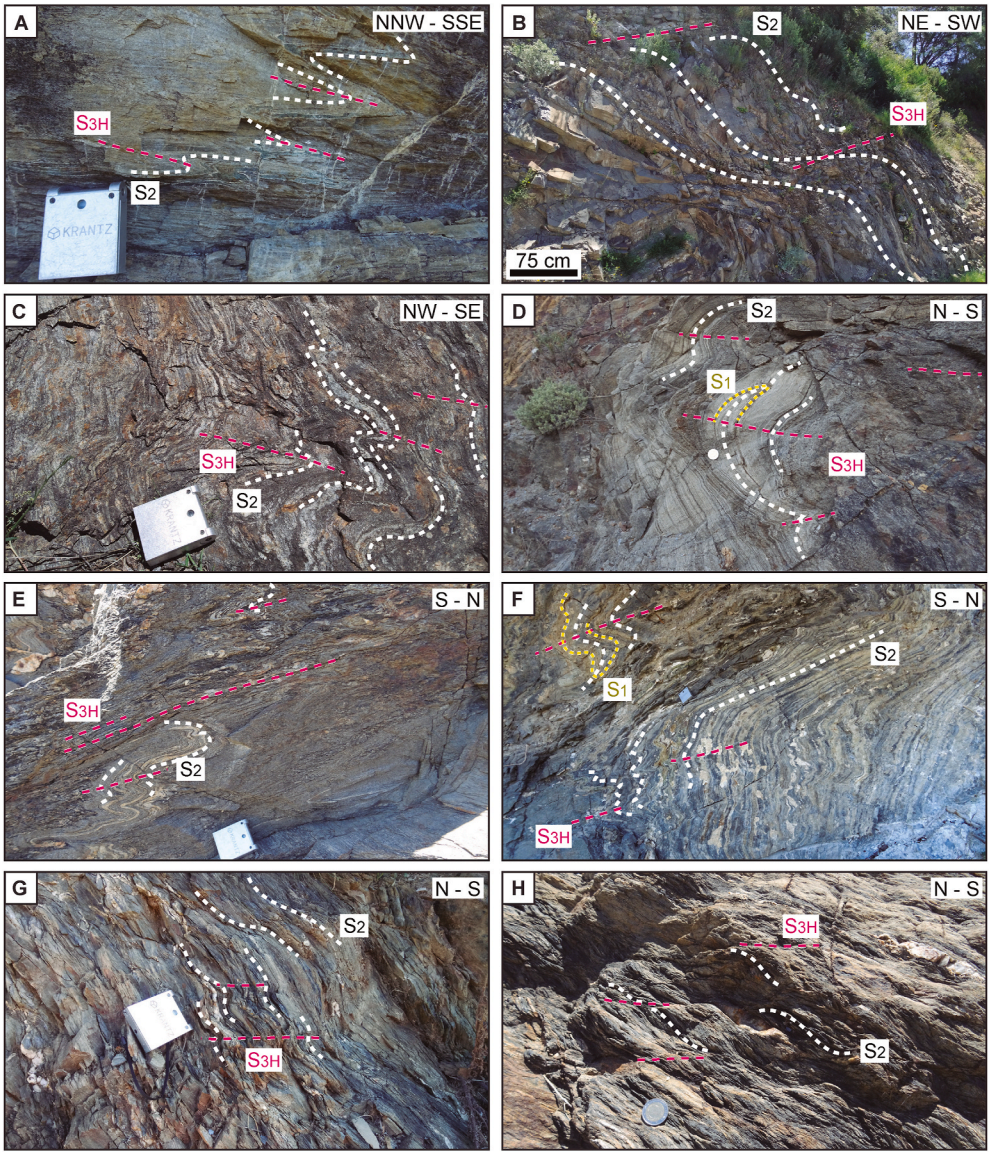

Fig. 4. Outcrop images of S_{3H}. A) Intensely developed S_{3H} in quartzites situated near the middle of the Jubrique schist-quartzite formation. B) Widely spaced shear bands in the lower levels of the same formation. C) F_{3H} folds in gneisses of the Jubrique Fm. D) Folds associated with S_{3H} in the Benalmádena area. E) S_{3H} near Torrox transposing S_2 in a pelitic layer above a less deformed psammitic layer showing F_{3H} folds. F) Interference of F_2 and F_{3H} folds near La Herradura. G) Coeval D_{3H} folds and shear bands in the Contraviesa area. H) Subhorizontal shear bands south of Albondón genetically related to S_{3H}.

S_{3V} or S_{3H} (Fig. 5g, h, 8b, 8c). As previously described by Cuevas (1991), S_{3V} is particularly well developed in the Upper Alpujárride unit (Adra nappe) cropping out in the south of the Contraviesa area. Within the Intermediate Alpujárride unit (Murtas nappe) further north, S_{3V} becomes scarcer as D_{3H} structures make their appearance (Fig. 8). The latter correspond to south-verging tight to open folds with subhorizontal axial planes and top-to-the north shear bands and faults which postdate D_{3V} structures (Fig. 4g, h and 5g). F_2 folds and L_2 lineation have variable plunges and plunge directions, ranging from SE to SW, and define a broad N–S maximum (Fig. 7). Plunge directions of F_{3V} and F_{3H} folds show an even larger spread from E to S to W with a weak E-W maximum. In several outcrops an E-W to NE-SW striking S_{3V} was observed deforming an older steeply WSW dipping foliation, and resulting in very steeply SW plunging fold- and crenulation axes. This is consistent with structural data of Azañón et al. (1997) from the eastern Sierra de la Contraviesa, which also show early NNE-SSW trending lineation and folds (their 'L_2') overprinted by ENE-WSW trending folds (their 'F_3'). Thus, the weakly bimodal distribution of D_2 and D_3 linear structures in the Contraviesa area probably reflects the superposition of ENE-WSW structures over older N–S ones. Note that equivalent structural data for the Tocón, Torrox and Fuengirola areas all exhibit similar bimodal trends (Fig. 7).

4. Microstructural analysis

4.1. Microstructural approach

A total of 140 samples of medium-to high-grade metapelites containing garnet, staurolite, plagioclase and/or andalusite porphyroblasts (Figs. 9 and 10) were studied in thin section to analyze mineral relationships and to select appropriate samples for further microstructural analysis in additional differently oriented thin sections and X-ray computed micro-tomographies (XCT) (see XCT method on Supplementary Material SM1). SM2 (Supplementary material) lists the 60 selected samples, their locations and corresponding nappe units. Fig. 11a shows the general relationships between the principle index minerals in these rocks and the traditionally distinguished deformation phases. Sillimanite is a good marker of the high-temperature stage in high-grade rocks linked to the D_2 event. Andalusite mainly grew during D_3 (Cuevas, 1989; Azañón et al., 1998; Williams and Platt 2017), although we actually recognized three different types of andalusite porphyroblasts: (i) small equidimensional crystals with well-developed straight to sigmoidal inclusion trails indicating syn-D_3 growth (Fig. 10c, d and e), (ii) up to several cm long post-kinematic crystals overgrowing all matrix fabrics (Fig. 10f), and (iii) large crystals usually devoid of inclusion trails

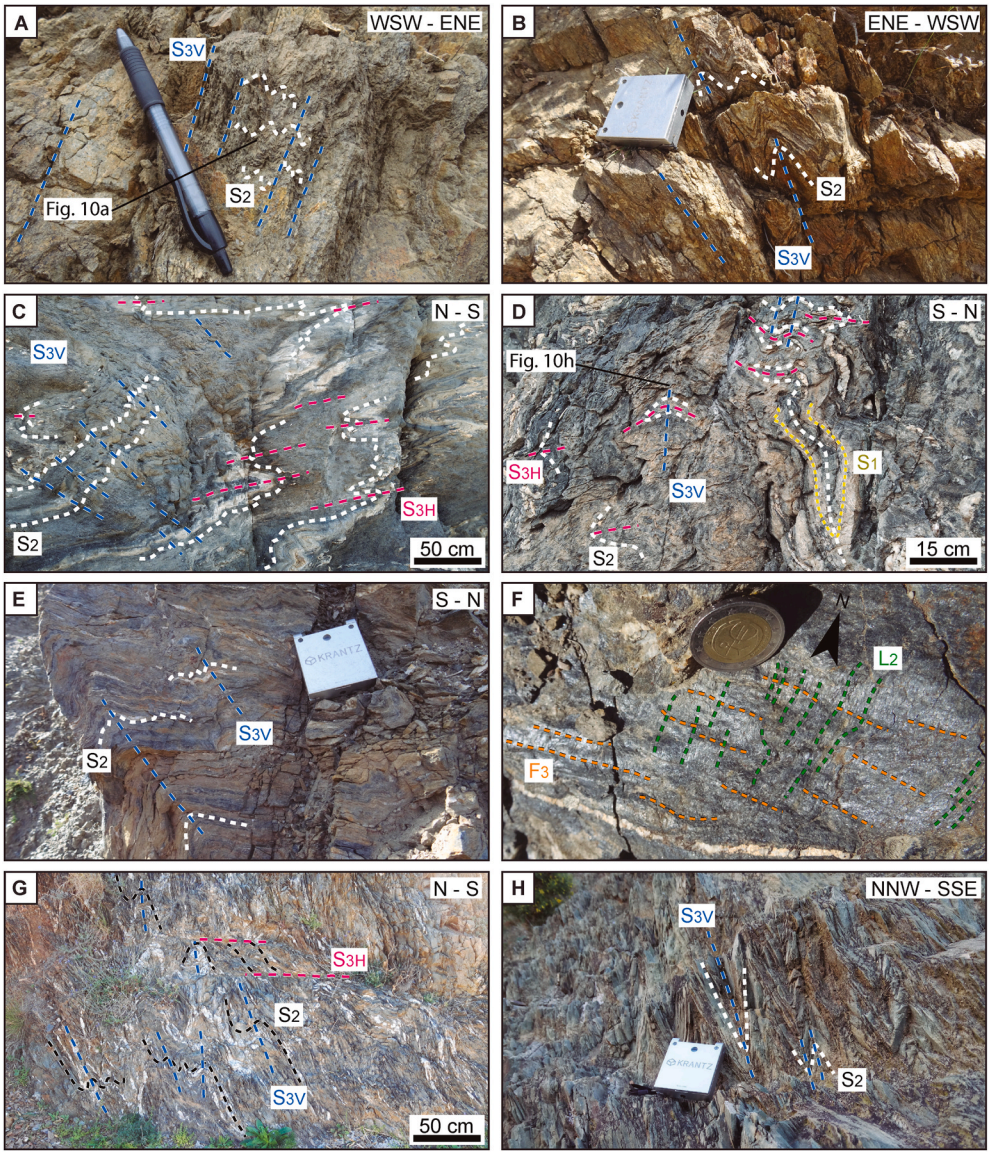

Fig. 5. Outcrop images of S_{3V}. A) S_{3V} is intensely developed and becomes the main foliation in outcrop south of Mijas. Fig. 10a shows a microscope image of the S_{3V} crenulations. B) Intensely folded gneisses south of Mijas. C) S_{3V} overprinting D_{3H} folds east of Almuñécar. Fig. 10b shows a microscopic image of the same outcrop. D) Fold interference in amphibolites of the Herradura nappe west of Almuñécar with S_{3V} overprinting S_{3H}, in turn overprinting an F_2 fold. Fig. 10h shows a microscope image of the same outcrop. E) South-vergent D_{3V} folds north of Tocón de Quéntar. F) N–S L_2 overprinted by E-W F_{3V} folds north of Tocón de Quéntar. G) D_{3V} folds cut by D_{3H} shear bands in the Contraviesa area. H) S_{3V} partially transposing S_2 in the Contraviesa area.

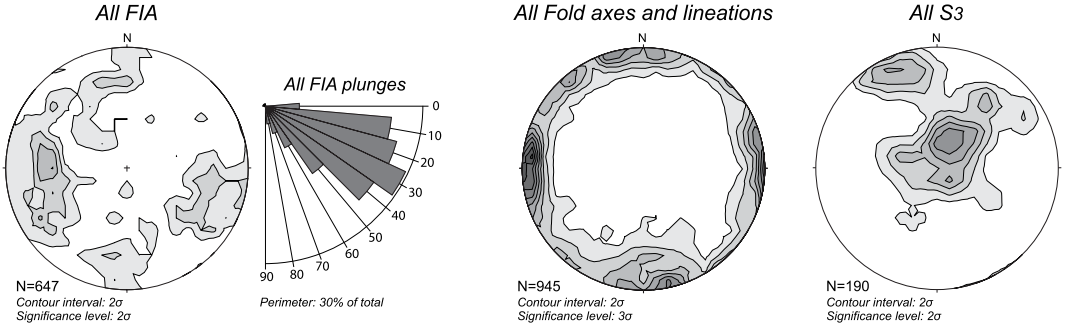

Fig. 6. Equal-area and lower-hemisphere projections for: total porphyroblast FIAs measured in all areas, all fold axes and lineations shown separately for different areas in Fig. 7, and a similar compilation of poles to all crenulation cleavages shown in Fig. 7. All equal-area projections were made with the program 'Stereonet' by Allmendinger et al. (2013) and use Kamb contours with contour interval and significance level set to 2 or 3σ (see figure).

which appear broken, stretched (Fig. 10g) and partially replaced by fine-grained quartz-mica aggregates. The third type possibly corresponds to the pre-Alpine andalusite crystals reported by Sánchez-Navas et al. (2012) in the vicinity of the Torrox orthogneiss.

Whilst garnet porphyroblasts in our samples of Permo-Triassic metasediments can only be Alpine, those in Paleozoic dark schists could, in principle, also be Variscan. Nevertheless, an Alpine origin in both rock types is considered likely because (i) evidence for Variscan garnet growth has previously only been found in high-grade gneisses not studied herein, (ii) inclusion trails of garnets in samples from cover and

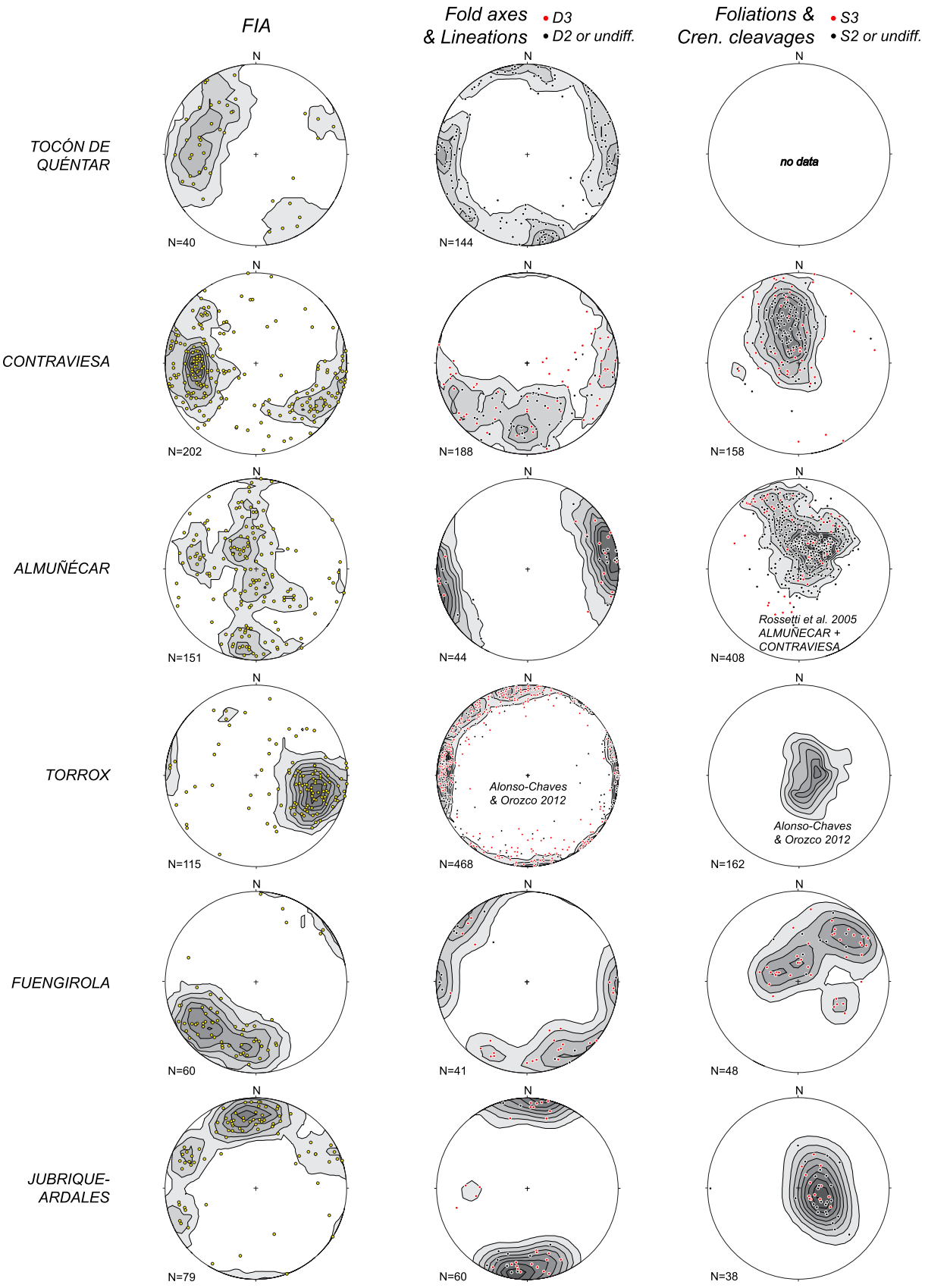

Fig. 7. Equal-area and lower-hemisphere projections for: porphyroblast FIAs measured in different areas, F_2/L_2 (black dots) and F_3/L_3 (red dots) fold axes and associated lineations measured in outcrop, and poles to the main foliation (S_2; black dots) and superposed crenulation cleavages (S_3; red dots). All equal-area projections were made with the program 'Stereonet' by Allmendinger et al. (2013) and use Kamb contours with both contour interval and significance level set to 2σ.

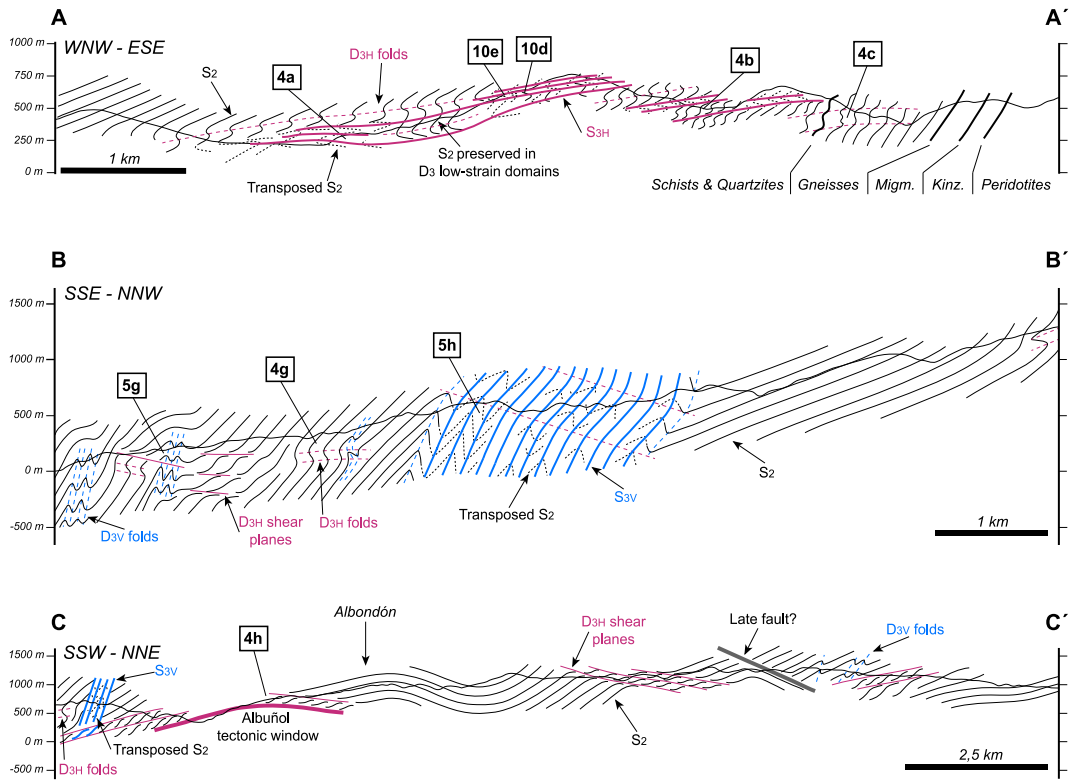

Fig. 8. Cross sections of the Jubrique (A-A′) and Contraviesa (B–B′ and C–C′) areas. White numbers in black squares correspond to Figure numbers.

basement rocks have similar orientations as shown further, and (iii) Sm–Nd ages of garnets in five Paleozoic schist samples from the Alpujárride- and Sebtide complexes are all Alpine (Farrell, 2019; Aerden et al., 2022).

The studied porphyroblasts host straight to weakly sigmoidal to spiral-shaped inclusion trails composed of quartz, graphite and/or opaque minerals (Figs. 9 and 10), although inclusion trails-free porphyroblasts are also common. Samples were initially studied in horizontal thin sections (regardless of the orientation of the matrix foliation and lineation), because of the advantage that the strike of relatively straight inclusion trails can be directly measured on such sections. Samples were classified in three groups. A first group of 36 samples contains garnet porphyroblasts with well-developed sigmoidal or spiral inclusions whose FIA can be readily measured in XCT scans. Some of these samples also contain planar inclusion trails whose orientations were also measured. A second group of 15 samples contains asymmetrically curved inclusion trails, but either less well developed in garnet porphyroblasts or well developed but hosted by other porphyroblastic minerals (andalusite, plagioclase, staurolite), which are less apt for XCT analysis because of a lower X-ray attenuation contrast with their mineral inclusions and the matrix. These samples were studied using the radial thin-sectioning technique of Hayward (1990) and Bell et al. (1995) by which the average orientation of porphyroblast FIAs in a sample can be determined. As we cut six vertical thin sections for each sample, our average FIAs are constrained to 30° trend ranges. A third group of 9 samples only contains porphyroblasts with relatively straight inclusion trails, whose strikes were measured in the initially cut horizontal thin sections. Microstructural data obtained from XCT scans and thin sections are presented in contoured equal-area projections made with 'Stereonet' (Allmendinger et al., 2013) and in moving-average rose diagrams, respectively, for each sample. The rose diagrams were made with the program 'MARD' (Munro and Blenkinsop, 2012). Due to space limitations, these diagrams are provided as supplementary data together with a table summarizing the mean microstructural orientation in each sample (Supplementary Material SM3, SM4 and SM5).

4.2. Relative timing criteria and microstructural sequence

Mean microstructural trends defined by FIAs and/or inclusion-trail strikes are plotted in rose diagrams for all porphyroblastic minerals collectively (Fig. 11b) and also separately for garnet versus plagioclase, andalusite and staurolite porphyroblasts (Fig. 11c). Three sets of microstructures are visible in these plots that define NNW-SSE (green), ENE-WSW (orange) and WNW-ESE (red) orientation maxima. Note that, whereas all three sets are present in garnet porphyroblasts, andalusite, staurolite and plagioclase porphyroblasts almost exclusively contain the NNW-SSE and ENE-WSW sets.

Relative timing criteria for microstructures with different trends include: (1) porphyroblasts with differently oriented FIAs in the core versus the rim (Fig. 12a and b), (2) porphyroblasts containing inclusion trails with different strikes in the core versus rim (Fig. 12c), (3) weakly crenulated inclusion trails whose axial planes can be taken as the direction of an incipient foliation (Fig. 12d), (4) inclusion trails hosted in garnet versus staurolite and andalusite, since the latter formed later (e.g. Balanyá et al., 1997; Azañón et al., 1997; Williams and Platt, 2017), (5) crenulation lineations in the matrix versus FIAs.

Fig. 11e summarizes timing relationships found in our samples following the above criteria. Mean microstructural trends are represented with red, orange or green symbols depending on their association with the WNW-ESE, ENE-WSW or NNW-SSE modal maxima in the rose diagram of Fig. 11b. In the case of a mean microstructural trend falling within the overlap zones between two trend groups its assignment to one of these groups was based on relative timing criteria with other microstructural trends in the sample or in nearby samples. The trends of matrix crenulations and fold axes measured in samples or their outcrops are also represented (star and triangle symbols).

Mutual relative-timing criteria between inclusion trails in porphyroblasts (five samples) suggest that WNW-ESE FIAs (red) formed first, followed by ENE-WSW FIAs (orange) and finally NNW-SSE ones (green). This succession is supported by the fact that matrix lineations and folds mainly have 'green' and 'orange' trends and that 'red' FIAs almost

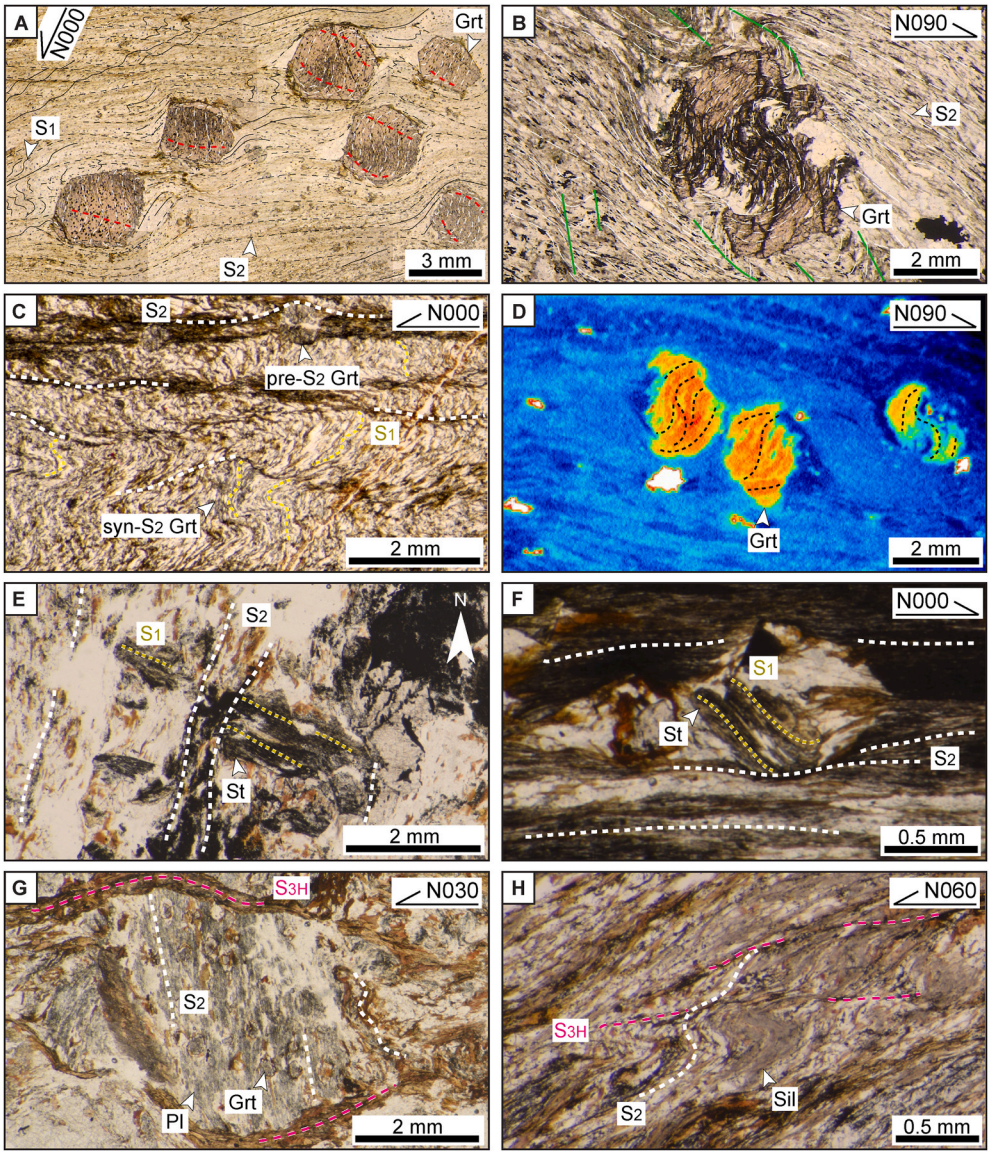

Fig. 9. Microstructural images (taken under plane polarized light except D which is an XCT image; half arrows indicate the upward direction together with the normal direction indicating the horizontal, geographic direction with numbers). A) Garnets with sigmoidal inclusion trails. The S_2 foliation and relics of S_1 are visible in the matrix. B) Garnet with sigmoidal inclusion trails with internal truncations. C) Syn-S_2 garnets of the Benamocarra unit in microlithons of an incipient S_2 foliation. D) XCT image of garnets hosting spiral shaped inclusion trails. Same sample as in B for comparison. E) Staurolite porphyroblasts whose straight inclusion trails are wrapped by S_2 (plain view, north is indicated by the arrow). F) Staurolite porphyroblast with weakly sigmoidal inclusion trails. G) Plagioclase with straight inclusion trails including tiny garnet porphyroblasts. H) S_{3H} folding sillimanite associated with S_2 in the Fuengirola area. Note local shear-band character of S_{3H}.

exclusively occur within garnet porphyroblasts (Fig. 11c), whereas the two younger FIA sets are found equally in garnet, staurolite, andalusite and plagioclase porphyroblasts. One sample (63.8.1) contains a 'red' FIA hosted by staurolite, which probably grew synchronous with garnets in other samples.

Sample 68.4.1, however, paradoxically contains a 'red' FIA included by late (syn-D_{3H}) andalusite porphyroblasts post-dating garnet growth. Two possible explanations are (1) that these andalusites grew in a zone where 'red' structural trends were preserved due to the partitioning of later deformations around it, or (2) grew in a pre-existing plunging fold which can create FIAs oblique to the shortening direction (see Fig. 5e of Aerden et al., 2022). Another contradictory relationship was found in sample 66.11.1, where garnets with 'green' FIAs are surrounded by L_2 lineation and F_2 folds oriented within the 'red' trend range (133/05). The proximity of this direction to the overlap zone with the 'green' trend range and the fact that neighboring sample 66.10.1 hosts similar matrix structures but trending slightly more NNW-SSE within the 'green' trend range suggests that 66.11.1 is an outlier and in fact belongs to the 'green' trend group. All other relative timing criteria between FIAs versus L_2 and F_2 folds are consistent with the sequence of 'red', 'orange' and 'green' microfabrics.

Relative timing relationships between FIAs and L_3 lineations and F_3 folds imply a repetition of 'orange' fabrics after 'green' ones. This follows from nine samples containing E-W to NE-SW trending L_3/F_3 surrounding inclusion trails with 'green' FIAs or strikes (Fig. 11e). Furthermore, syn-D_3 andalusite porphyroblasts preserve both 'green' and 'orange' FIAs that necessarily post-date all garnet FIAs and S_2. Indeed, both S_{3H} and S_{3V} matrix crenulations deform sillimanite fibers associated with S_2 (Figs. 9h, 10a and 10b, 10c and 11a; Cuevas 1989; Azañón et al., 1998; Williams and Platt 2017)

4.3. Regional distribution of microstructural trends

FIAs, lineations and fold axes in our samples and their outcrops are shown in the maps of Figs. 2 and 3 with red, orange or green trend bars. The curvature sense or asymmetry of sigmoidal to spiral-shaped inclusion trails is symbolized in these maps with small arrows drawn normal to FIA trend bars. These arrows are opposite to the direction of tectonic transport that would be traditionally deduced from the asymmetry of inclusion-trails, assuming a 'rotational' origin, but point in the correct direction according to the non-rotational interpretation (Bell and Johnson, 1989) favored in this paper (see section 5.1). For ease of discussion, inclusion-trail asymmetries are therefore specified in terms of tectonic transport directions predicted by the 'non-rotational' model.

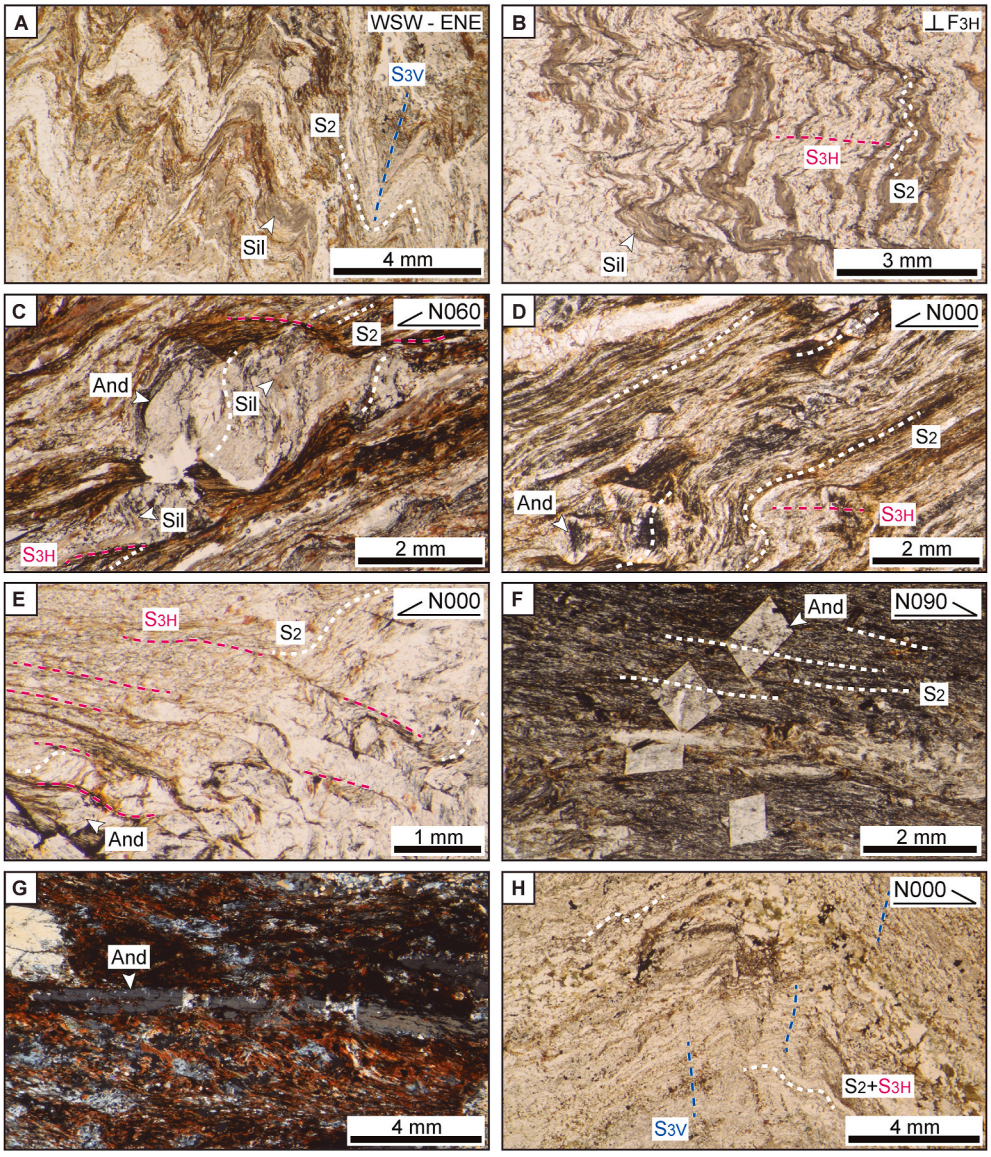

Fig. 10. Microstructural images (taken under plane polarized (A, B, C, D, E, F, H) or cross polarized light (G); half arrows indicate the upward direction together with the normal direction indicating the horizontal, geographic direction with numbers). A) Detail of outcrop image of Fig. 5a. Sillimanite is folded by S_{3V}. B) Detail of outcrop image of Fig. 5c. S_{3H} crenulates a sillimanite-bearing S_2. C) Syn-D_{3H} andalusite porphyroblasts include sillimanite-bearing S_2. D) Syn-D_{3H} andalusite porphyroblasts of the Jubrique area. E) S_{3H} partially transposes S_2 and is associated with andalusite growth. Jubrique area. F) Post-kinematic andalusite porphyroblasts of the Tocón de Quéntar area. G) Stretched andalusite porphyroblast adjacent to the Torrox gneiss which might be Variscan. H) Incipient S_{3V} affects S_2 and S_{3H} in the outcrop of Fig. 5d.

That is, a clockwise sigmoid or spiral corresponds to top-to-the right tectonic transport.

Different FIA sets are heterogeneously distributed in the Alpujárride complex. In the Western Betics (Fig. 2a) only 'green' and 'orange' FIAs have been found in 14 samples with the exception of sample 70.6.1, which contains both 'orange' and 'red' FIAs. Particularly noteworthy is the consistency of FIA orientations in the Fuengirola and Jubrique areas despite very different trends of matrix lineations and fold axes in both regions (E-W to SE-NW versus N–S, respectively). In the Almuñécar-Torrox area (Fig. 2b), significant differences can be noticed between the data from samples collected west and east of Nerja. West of this town, garnets mainly preserve 'red' and 'green' FIAs, whereas east of it all three FIAs are roughly equally represented and this is further maintained to the east in the Tocón de Quéntar and Contraviesa areas (Fig. 3a and b).

5. Interpretation and discussion

5.1. Formation mechanism of inclusion trails

Consistent inclusion-trail orientations in metamorphic belts (see Introduction) have been mostly explained in terms of a model envisaging porphyroblast nucleation and growth within actively developing microlithon domains without much porphyroblast rotation (Bell, 1985; Fay et al., 2008; Bell and Fay 2016). According to this model, sigmoidal and spiral-shaped inclusion trails form by overgrowth of one or multiple crenulations. Furthermore, preferred subvertical and subhorizontal orientations of inclusion trails documented in different orogens (Bell et al., 1992; Hayward, 1992; Johnson, 1992; Aerden, 1994, 1995, 1998, 2004; Mares, 1998; Sayab, 2005; Shah et al., 2011; Bell and Sapkota, 2012; Aerden et al., 2013; Aerden and Ruiz-Fuentes, 2020) are inferred to reflect alternations of crustal shortening and transient gravitational collapse stages. FIAs resulting from this process should have subhorizontal plunges and trends normal to the crustal shortening direction.

Several general features of our microstructural data, and similar ones described by Aerden et al. (2022, their Fig. 6) support the above summarized 'non-rotational' model in the Betic-Rif orogen and its predictions:

- Our FIAs have mainly sub-horizontal to gentle plunges regardless of their trend or timing (Fig. 6). If they had formed by shearing-induced porphyroblast rotation, then it is difficult to explain why older FIAs

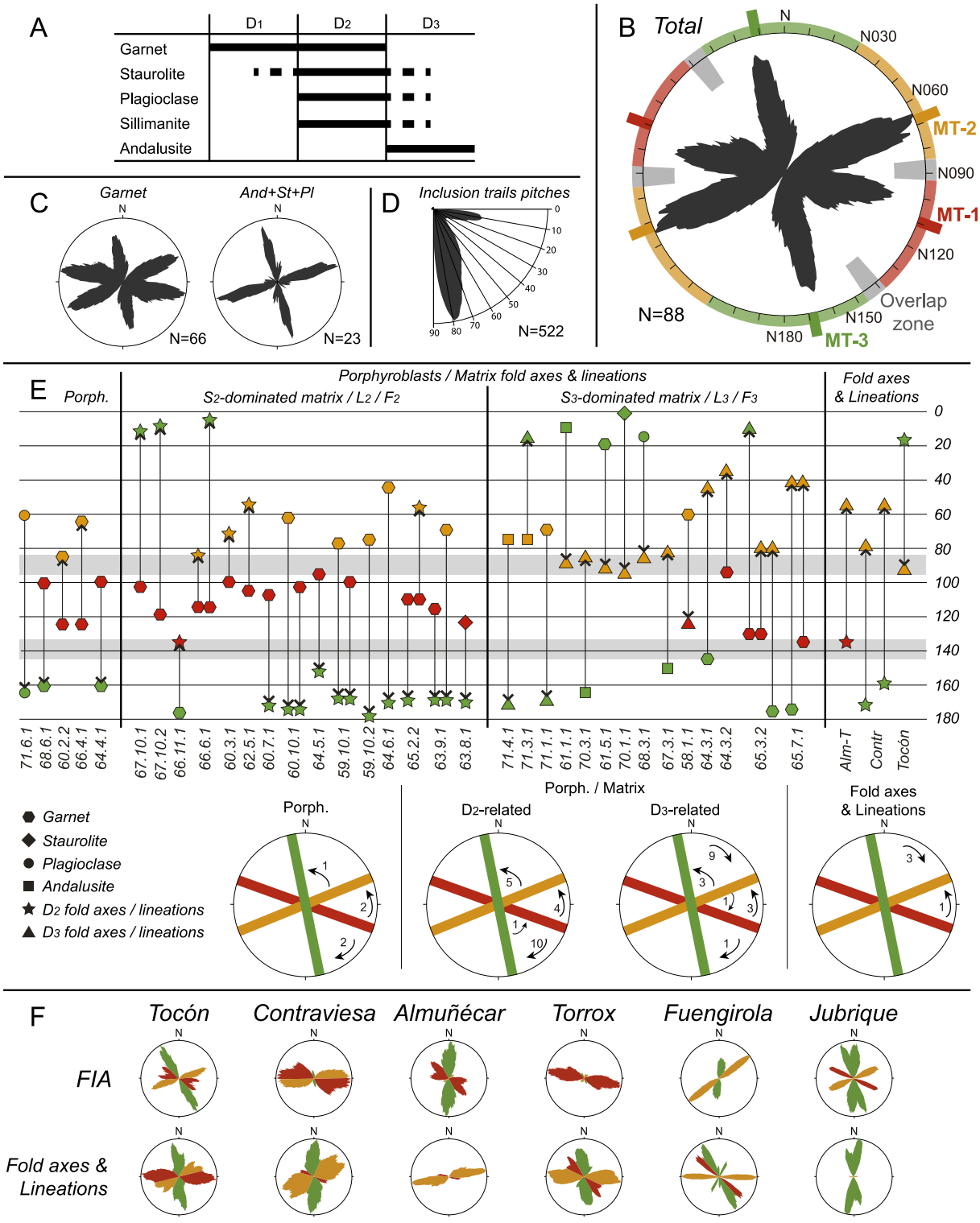

Fig. 11. A) Summary of relationships between mineral growth and deformation phases. B) Rose diagram compiling all mean FIA trends and inclusion-trail strikes listed in SM5. Three microstructural trends (MT-1, MT-2 and MT-3) are indicated associated with modal maxima at N070, N110, N170 and trend ranges N140–N090, N090–N030, N140–N210. Structures falling within these trend ranges are colored red, orange and green, respectively, in E and F. C) Same data separated for garnets versus andalusite, staurolite and plagioclase. D) Summary of inclusion trail pitches measured in sections oriented normal to FIA in samples containing a single or very dominant FIA set. Data from individual samples can be found in SM6. E) Temporal relationships between (micro)structures with different trends in individual samples based on inclusion-trail geometry alone (core-rim relationships, truncational relationships, crenulated inclusion trails), inclusion trails versus crenulation- and fold axes in the matrix (S_2 and S_3 dominated), and overprinting relationships between fold axes and lineations mutually. Arrows point from older to younger elements and are summarized by four circular diagrams, where numbers indicate how many times each temporal relationship is found. F) Rose diagrams for FIAs, fold axes and lineations plotted in Fig. 7 and color-coded according to the three trend ranges defined in B. (For interpretation of the references to color in this figure legend, the reader is referred to the Web version of this article.)

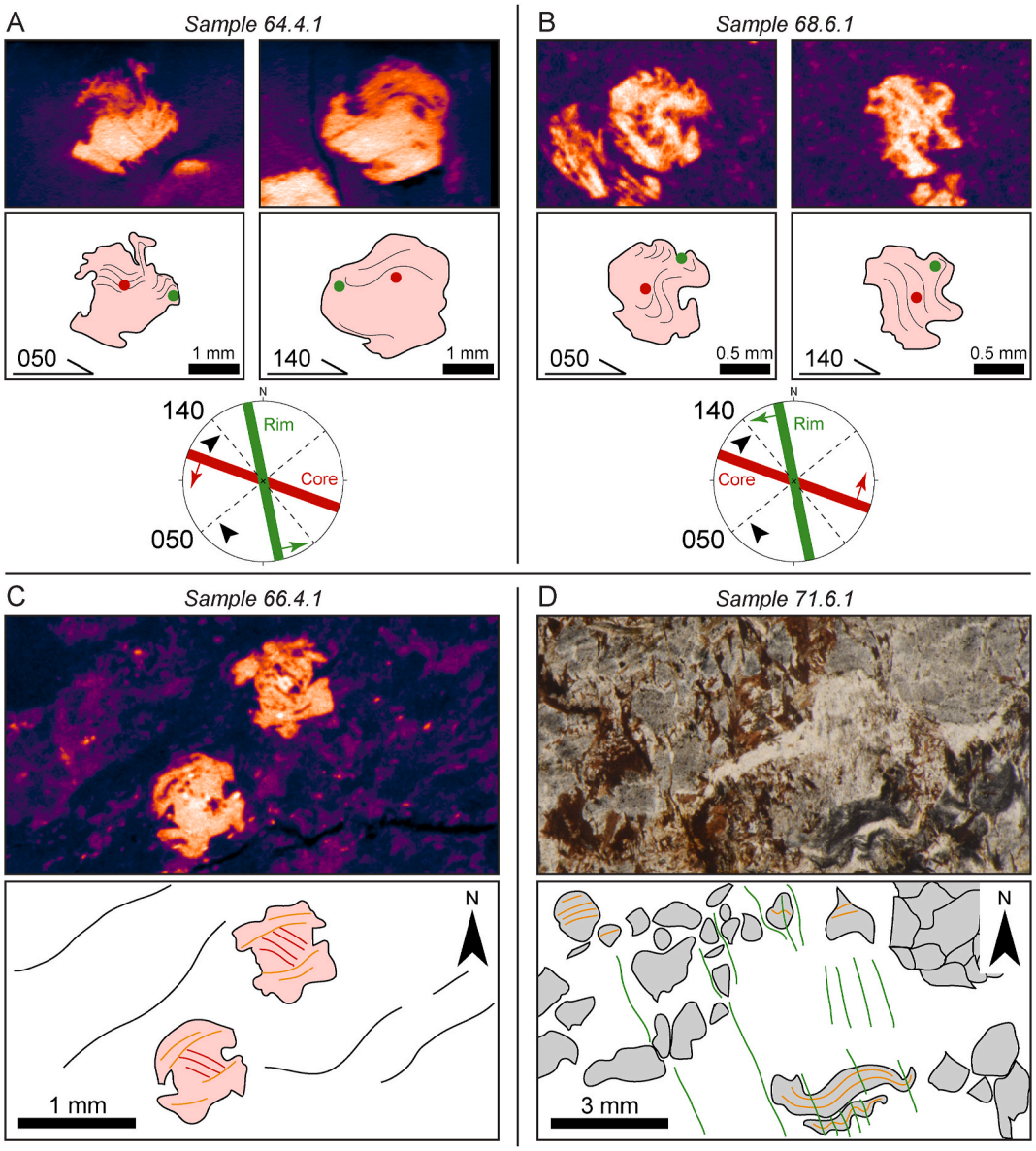

Fig. 12. Examples of temporal relationships between microstructural trends indicated by different FIAs (A and B; XCT images; half arrows indicate the upward direction together with the normal direction indicating the horizontal, geographic direction with numbers), different inclusion-trail strikes (C; XCT image; plain view, north is indicated by the arrow) in core versus rims of garnets, or by weakly crenulated inclusion trails (D; microphotograph, plane polarized light; plain view, north is indicated by the arrow) in plagioclase. The microstructural trends are color-coded according to the three trend ranges defined in Figure 11b.

were not reoriented and steepened during the development of younger ones.

- Dip angles of internal foliations measured in porphyroblast cores show a bimodal distribution with strong preferences for steep or flat lying (Figs. 11d and 13 and SM6). Axial planes and truncations associated with more complex inclusion-trail patterns exhibit similar flat-steep patterns (Fig. 13).
- FIA trends have consistent orientations in samples and areas where matrix structures and fabrics have totally different orientations (Fig. 2a).
- The shear sense indicated by asymmetric pressure shadows of porphyroblasts often conflicts with the sense of inclusion-trail curvature if porphyroblast rotation is assumed (Fig. 14).

5.2. Kinematic significance of 'S_1' inclusion trails

Williams and Platt (2017) already noted that garnet porphyroblasts occasionally host crenulated inclusion trails, which imply a polyphase character of 'D_1'. The three sets of inclusion trails distinguished in this paper suggest a superposition of three regional-scale kinematic frames further referred to as D_{1A}, D_{1B} and D_{1C} (Fig. 15). Aerden et al. (2022) recently recognized the same three FIA sets based on microstructural data that included 150 individual FIAs measured with XCT in 12 samples of the Sebtide Complex (the African equivalent of the Alpujárrides), another 150 individual FIAs in five samples of the Nevado-Filábride Complex complemented with 87 average FIAs for the Nevado-Filábride Complex, but only 47 individual FIAs from seven samples of the Alpujárride Complex. Our expansion of the data for the latter to 647 individual FIAs plus 25 average FIAs from 60 samples confirms the orogen-wide character of the three FIA directions and supports a relationship with the plate motion history of the Mediterranean Alpine belt proposed by Aerden et al. (2022).

These authors showed, based on Sm–Nd garnet ages and published plate-motion reconstructions (Rosenbaum et al., 2002; Vissers and Meijer, 2012; DeMets et al., 2015), that the 'red' FIA set (D_{1A}) probably formed in the latest-Eocene to early Oligocene perpendicular to NNE

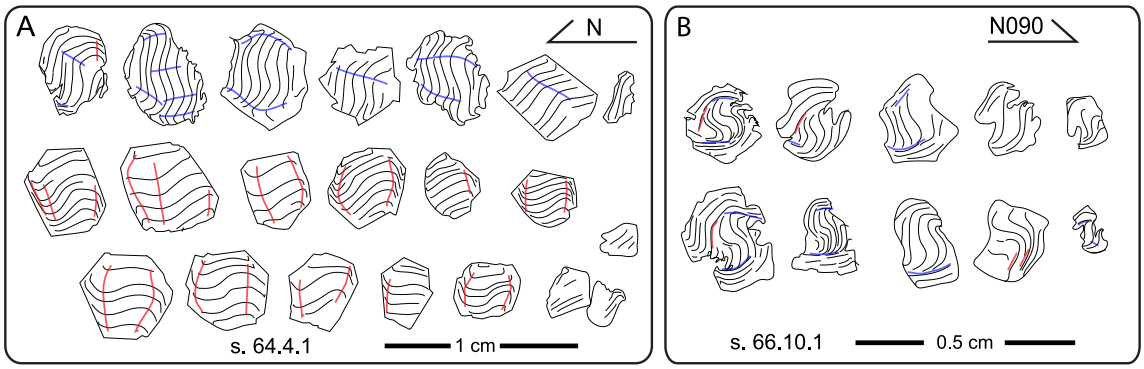

Fig. 13. Line tracings of inclusion trails drawn on high-resolution microphotographs of vertical thin sections oriented approximately normal to porphyroblast FIAs. Half arrows indicate the upward direction together with the normal direction indicating the horizontal, geographic direction with numbers. A) Inclusion trails in sample 64.4.1 exhibit subhorizontal (blue lines) and subvertical (red lines) axial planes, consistent with the garnets having nucleated at least twice during different crenulation forming events related to crustal shortening and collapse. B) Complex sigmoidal and spiral shaped inclusion trails in sample 66.10.1 associated with internal truncations (blue and red lines). These elements show similar preferred orientations as the axial planes in A, consistent with episodic growth pulses of individual porphyroblasts controlled by contraction-collapse cycles (e.g. Bell and Hayward, 1991). (For interpretation of the references to color in this figure legend, the reader is referred to the Web version of this article.)

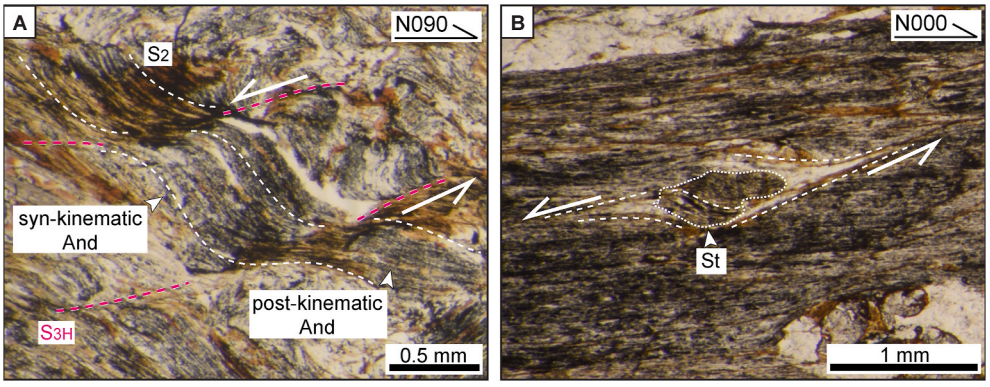

Fig. 14. Andalusite (A; sample 70.3.1) and staurolite (B; sample 64.6.1) porphyroblasts containing weakly sigmoidal inclusion-trails that have the same asymmetry as shear bands and strain shadows (microphotographs taken under plane polarized light; half arrows indicate the upward direction together with the normal direction indicating the horizontal, geographic direction with numbers). Note that this is consistent with a 'non-rotational' interpretation of the inclusion trails as overgrown crenulations.

directed motion of Africa relative to Eurasia. Subsequent 'orange' FIAs (D_{1B}) dated between 27Ma and 22Ma in the Alpujárride-Sebtides would have developed during or after an anticlockwise rotation of the plate-motion vector to NW. The third set of 'green' FIAs (D_{1C}) was attributed to westward extrusion of the Alborán Domain in the early Miocene, approximately normal to Africa-Iberia convergence.

Aerden et al. (2022) also speculated about the polarity of subduction as suggested by the curvature sense or asymmetry of inclusion trails (see below). However, their asymmetry data were limited to 14 samples of the Sebtide Complex, six from the NFC and only four from the Alpujárride Complex. Our extension of this data to 42 Alpujárride samples now allows statistically more significant conclusions. Fig. 16 shows the asymmetries recorded in samples from different areas of the Alpujárride and Sebtide complexes. Of 25 samples hosting D_{1A} FIAs, 13 exhibit top-SSW asymmetries, 9 top-NNE, and 3 contain porphyroblasts showing opposite asymmetries (Figs. 2 and 3). The top-NNE asymmetries mainly correspond to the Benamocarra unit as mapped by Williams and Platt (2018) and the Intermediate Alpujárride unit (Herradura nappe). In the Upper Alpujárride units (Adra and Salobreña nappes) and the Sebtides, D_{1A} asymmetries very consistently indicate top-SSW transport thus favoring a northward dipping subduction zone (Figs. 16 and 17). The asymmetries of D_{1B} (orange) FIAs also exhibit a strong predominance (Fig. 16; 19 to 7) of top-S to -SE, which is consistent with generally accepted NW-dipping subduction of the African plate below the Alborán domain in the late Oligocene to early-Miocene (Fig. 17). Interestingly, the asymmetry of D_{1B} FIAs recorded in two Benamocarra samples are again opposite (top-NW) to that in the underlying Upper Alpujárride unit. The third set of inclusion-trails (D_{1C}) has a top-west asymmetry in 11 samples, top-east asymmetry in 11 samples and opposite asymmetries in 3 samples. This may reflect distributed coaxial shortening in the Alpujárride complex driven by westward migration of the Alborán Domain in the Miocene without a dominant vergence.

The predominance of gentle FIA plunges and the bimodal steep-flat orientations of inclusion trails detected in our samples (Figs. 6, 11 and 13 and SM6) implies an unspecified number of alternations between crustal shortening and transient gravitational instability (collapse) during D_{1A}, D_{1B} and D_{1C}. Presumably these reflect fluctuations in a critical balance between tectonic stresses and gravity controlled, in turn, by variations in the rates of erosion, uplift, and plate convergence, the thermal and rheological evolution of the orogen and changes in boundary conditions. Intermittent collapse phases during D_1 must have been relatively weak compared to shortening phases as they are not reflected in cyclic prograde-retrograde metamorphism. Collapse events may correspond to gravitational spreading within thrust nappes in an overall contractional setting, alternating with periods of distributed shortening. In any event, these alternations were sufficient to control episodic growth of porphyroblasts with each growth pulse being triggered by a newly developing subvertical or subhorizontal crenulations (cf. Bell and Hayward, 1991; Sanislav and Bell, 2011; Aerden and Ruiz-Fuentes, 2020). This mechanism also explains the preponderance of subhorizontal or gently plunging FIAs.

Two samples from the Almuñécar area (66.9.1 and 62.5.2), however, contain very steeply plunging FIAs (Fig. 7 and SM3) corresponding to the intersection of two steeply dipping foliations with different strikes

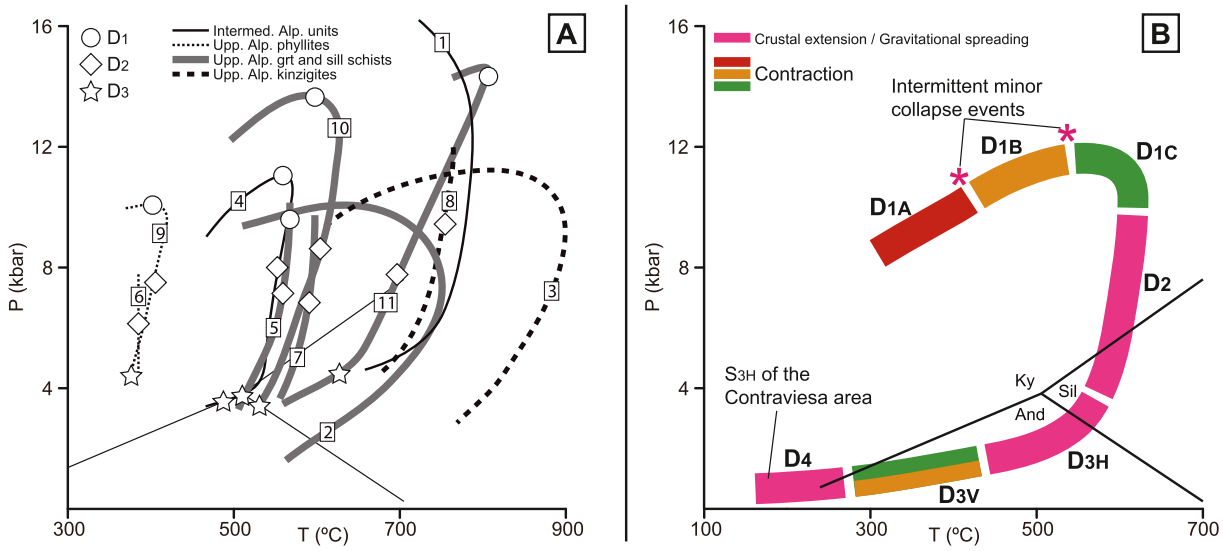

Fig. 15. A) P-T-t paths of different tectonic units of the Alpujárride complex. The conditions of the rocks studied in this work correspond to garnet-sillimanite schists of the Upper Alpujárride units. The paths of phyllites and kinzigites of the Upper Alpujárride units, and of the Intermediate Alpujárride units are also shown for comparison. Circles, squares and stars show the approximate location of deformation phases along the path as interpreted by the original authors. (1) Eclogites of the Ojén nappe (Tubía and Gil-Ibarguchi, 1991); (2) sillimanite schists of the Los Reales nappe near Fuengirola (Tubía, 1994); (3) kinzigites of the Los Reales nappe near Fuengirola (Tubía, 1994); (4) light colored schists of the Tejeda unit, equivalent to Intermediate Alpujárride units or Herradura nappe (Azañón and Alonso-Chaves, 1996); (5) garnet schists of the Adra nappe (Azañón et al., 1997); (6) phyllites of the Jubrique unit (Balanyá et al., 1997); (7) sillimanite schists of the Jubrique unit (Balanyá et al., 1997); (8) kinzigites of the Jubrique unit (Balanyá et al., 1997); (9) phyllites of the Salobreña nappe (Azañón et al., 1998); (10) sillimanite schists of the Salobreña nappe (Azañón et al., 1998); (11) Bentomiz unit, Upper Alpujárride nappe from the Torrox area (Alonso-Chaves and Orozco, 2007). B) Schematic P-T-t trajectory for the higher grade (sillimanite bearing) rocks studied in this work based on A. The timing of deformation events distinguished in this work are tentatively indicated using the same colors (red, orange, green) as attributed in Fig. 11 to differently oriented structures. Gravitational collapse stages are colored in pink. (For interpretation of the references to color in this figure legend, the reader is referred to the Web version of this article.)

		Upper Alpujarride units and Lower Sebtides								*Intermed. Alp. units*	*Benamoc. unit*
		Jub.	Fueng.	Nerja-W	Nerja-E	Tocón	Cont.	Rif	Total		
D1A	top-NNE	1	0	0	0	1	1	1	4	2	3
	top-SSW	0	0	0	3	0	7	3	13	0	0
	both	0	0	0	0	1	0	1	2	0	1
D1B	top-NW	1	1	1	0	1	0	2	5	0	2
	top-SE	2	1	5	2	1	5	5	16	3	0
	both	0	0	0	0	1	0	0	1	0	0
D1C	top-W	1	2	3	0	0	0	2	8	2	1
	top-E	2	1	0	0	3	4	0	10	1	0
	both	0	0	0	1	0	1	0	2	0	1

Fig. 16. Table summarizing the asymmetries of inclusion trails from garnet, staurolite and plagioclase found in each area studied (Upper and Intermediate Alpujárrides and Benamocarra unit) and the Rif (in northern Morocco).

not separated by a flat lying crenulation cleavage. In the same area, straight inclusion trails which define internal foliations with steep dips are particularly abundant (samples 66.6.1, 60.2.2, 60.3.1, 66.4.1) possibly reflecting more limited role of gravitational collapse in comparison with other areas.

5.3. Kinematics of S_2

Even in individual thin sections, the character of the main cleavage varies from a differentiated S_2 crenulation cleavage deforming S_1 in the shortening field of D_2 to a simple schistosity that can be followed into garnet porphyroblasts and represents an S_1 that was deformed and reactivated in the extensional field of D_2. This composite character of the 'main foliation' and the fact that the process of foliation reactivation involves antithetic shearing (cf. Bell et al., 1986; Aerden, 1994) may explain partially contradictory shear-sense indicators associated with S_2. Nevertheless, most workers have concluded top-to-the-East to -NNE tectonic transport during D_2 with a component of coaxial shortening normal to S_2. The development of S_2 was accompanied by strong decompression related to opening of the western Mediterranean back-arc basin leading to sillimanite growth in the higher-grade rocks. Such an extensional origin of S_2 suggests it formed in a subhorizontal position although we have no firm data confirming this. This event (Fig. 17) is related with high-Temperature metamorphism dated at approximately 20 Ma (e.g. Platt and Whitehouse, 1998; Platt et al., 2005; Bessière et al., 2022), which is also the age of the oldest unconformable marine deposits on top of the Internal Domain (Viñuela Group, e.g. Aguado et al., 1990; Alonso-Chaves and Rodríguez-Vidal, 1998) and in the Alborán basin (Comas et al., 1992; Rodríguez-Fernández et al., 1999).

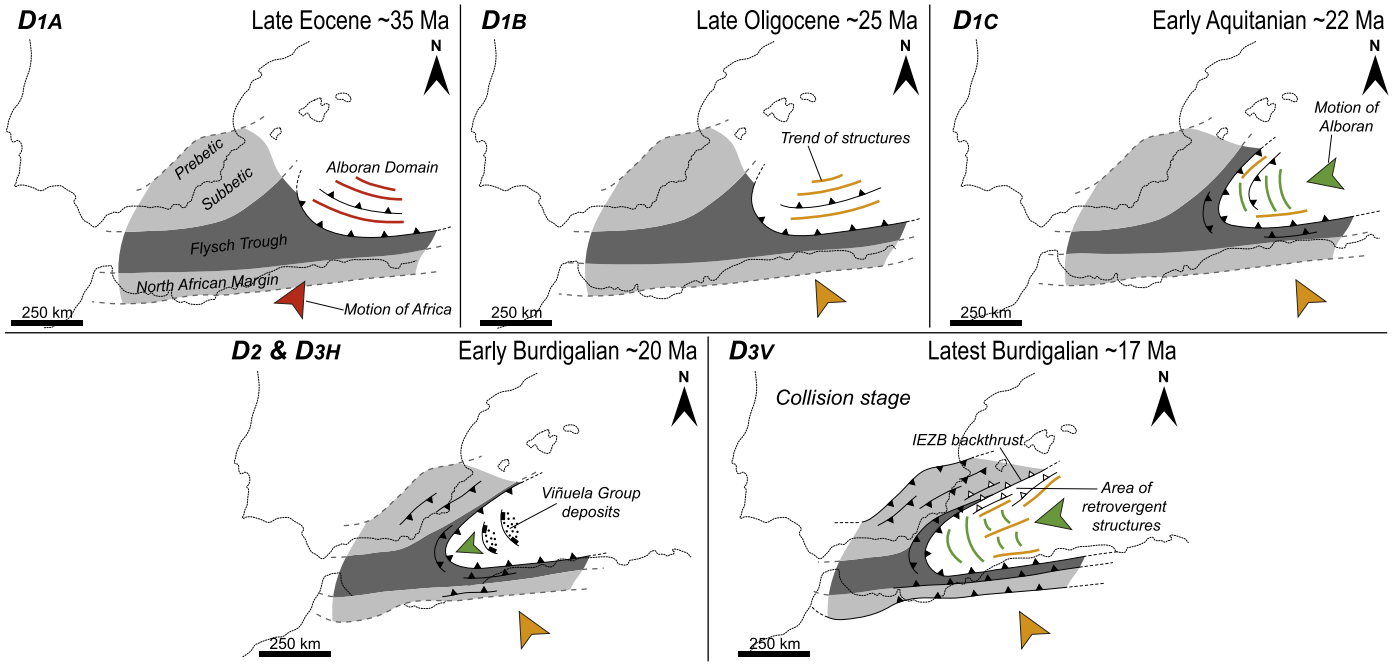

Fig. 17. Paleogeographic maps showing the evolution of the Alborán Domain in each phase distinguished in this study.

5.4. Kinematics of D_3

The tectonic significance of major N- to NW verging F_3 folds in the Alpujárride Complex and associated S_3 crenulation cleavage has been debated since long. In the Central Betics, some authors interpreted these structures as late-metamorphic N-to NE-directed folds and thrusts following D_2 extension (Cuevas, 1991; Simancas and Campos, 1993; Azañón et al., 1997; Balanyá et al., 1997; Rossetti et al., 2005; Simancas 2018). Others envisaged their development during continued crustal extension but with a changed top-N shear sense (Orozco et al., 1998, 2004, 2017; Williams and Platt, 2018). In the Fuengirola area, Tubía et al. (1993) and Tubía (1994) interpreted D_3 as a phase of ESE-WNW sinistral transtension changing to ENE-WSW sinistral transpression. Orozco et al. (1998) and Rossetti et al. (2005) locally recognized two crenulation cleavages (corresponding to our S_{3V} and S_{3H}) and Sanz de Galdeano (1989) described a superposition of two E-W and N–S folding directions in Triassic marbles of the Sierra de Tejeda (North of the Torrox area; Fig. 2b) both deforming an original 'main schistosity'.

Our own observations regarding D_3 can be summarized as follows (Figs. 15 and 17). In the Western and Central Alpujárrides (Jubrique, Fuengirola and Almuñécar areas), a penetrative S_{3H} is associated with synkinematic andalusite or sillimanite and is overprinted by late- to post-metamorphic S_{3V} (Fig. 5c, d, 10a, 10b). In the Contraviesa area, an opposite situation is found with steeply south-dipping S_{3V} locally overprinted by a gently dipping S_{3H} and post-metamorphic shear bands. The latter corresponding to the 'D_4' structures of previous workers. In the intermediate Torrox-Almuñécar area, S_{3H} is still the dominant crenulation cleavage but less intense as in the Jubrique schists and locally overprinted by D_{3V}. Thus, a west-ward strain gradient associated with S_{3H} is suggested. D_{3V} has only been found pervasively developed in the Fuengirola and Contraviesa areas. In the latter, zones of intense S_{3V} and tight folding of S_2 alternate with zones with a simple steeply south dipping S_2. Cuevas (1991) interpreted the intense D_{3V} folded zones as ductile thrusts supported by quartz c-axes fabrics indicating top-NE shearing.

These heterogeneous relationships suggest that, following several alternations of crustal shortening and weak gravitational collapse stages that generated the three FIA sets preserved in garnets (D_1), a more dramatic collapse event occurred (D_2 and D_{3H}) related to opening of the western Mediterranean basin that was still followed by renewed crustal shortening responsible for S_{3V}. The late subhorizontal shear bands and detachments (D_4 of previous workers) may reflect a final phase of thrusting and gravitational spreading following uplift caused by D_{3V} (cf. Platt et al., 1983). Interestingly, several authors already interpreted D_1-D_4 in terms of alternating shortening and extension (Tubía et al., 1993; Azañón et al., 1997, 1998; Balanyá et al., 1997). Such a scenario appears confirmed and refined by our work.

The fact that 'green' and 'orange' FIAs of andalusite porphyroblasts must have formed after 'green' FIAs of garnets, and that 'green FIAs' in both minerals are surrounded by 'orange' D_3 fabrics in several samples was stated in section 4.2 as implying development of 'orange' FIAs before and after 'green' FIAs. We suggest that this reflects an alternation of two suborthogonal shortening directions related to NW motion of Africa and simultaneous westward motion of the Alborán Domain. Regional fold trends also define two sets with E-W and N–S to NW-SE trends in all investigated areas (Fig. 7). In the westernmost part of the Gibraltar arc the N–S set is dominant (Fig. 1), whereas towards the east E-W to NE-SW trends become more important (Balanyá and García-Dueñas, 1987; Balanyá, 1991; Balanyá et al., 2007).

5.5. Back-thrusting development

In the Tocón de Quéntar and Sierra de Baza areas, E-W trending D_{3V} folds are S-vergent, opposite to similar structures in the Almuñécar and Contraviesa areas. South-vergent structures have been previously also recognized in Sierra de Baza (Comas et al., 1979; Delgado Salazar et al., 1980), Sierra de las Estancias (Akkerman et al., 1980), Sierra de Almagro (García-Tortosa et al., 2002; Booth-Rea et al., 2005), Sierra de Carrascoy (Sanz de Galdeano et al., 1997) and in the Orihuela Mountains (Martín-Rojas et al., 2007) (see locations in Fig. 1). S-vergent D_3 folds are concentrated near the Internal-External Zones Boundary (IEZB), which represents the suture of the collision between the Alborán Domain and the South Iberian paleomargin. Farther to the south in our study areas, E-W trending folds are mainly north-vergent. In the northeastern part of the cordillera, the IEZB has been interpreted as a backthrust (Geel, 1973; Martín-Algarra, 1987; Jabaloy-Sánchez et al., 2007) with top-to-the-SSE/SE sense of movement (Lonergan et al., 1994). Back-thrusts have also been recognized in the Flysch Complex, Frontal Units and Maláguide Complex (Foucault, 1976; García-Dueñas and Navarro-Vilá, 1976; Rodríguez-Fernández, 1982; Martín-Algarra, 1987; Balanyá, 1991; Sanz de Galdeano et al., 1995; Geel and Roep, 1998; Fernández-Fernández et al., 2007; Martín-Algarra et al., 2009; Jabaloy-Sánchez et al., 2019a; Ruiz-Fuentes et al., 2022). The appearance of S-vergent D_{3V} folds in the Alpujárride Complex close to the IEZB can therefore be interpreted in terms of propagation of deformation associated to back-thrusting within the Alborán Domain acting as the backstop. These observations allow us to correlate D_{3V} with the beginning of the collision of Alborán with the External Domain, which accounted around the late Burdigalian (e.g. Martín-Algarra, 1987; Martín-Martín et al., 1996; Ruiz-Fuentes et al., 2022).

6. Conclusions

- Porphyroblasts in the Alpujárride Complex preserve a succession of three differently oriented FIA sets (WNW-ESE, E-W to NE-SW and NNW-SSE) defined by sigmoidal or spiral-shaped inclusion trails. The regional consistency of these microstructures and their preference for subhorizontal or gentle plunges, support the view that FIAs correspond to the intersections of steeply dipping and subhorizontal foliations formed during alternating crustal shortening and gravitational collapse (Bell and Johnson, 1989).
- The above implies that FIAs formed normal to crustal shortening directions and have conserved their original orientations throughout the subsequent orogenic evolution. This is shown to be consistent with the Paleogene-Neogene history of relative plate-motions between Africa, Iberia and the Alborán Domain. A major change from NNE-to NW-directed motion of Africa in the Oligocene (e.g. DeMets et al., 2015) accounts for the two earliest formed FIA sets. The third FIA is attributable to independent westward motion of the Alborán Domain since the early Miocene.
- A strong predominance of inclusion-trail asymmetries (curvature senses) associated with the first two FIA sets indicating top-SSW to top SE tectonic transport, favors a northward to NW-dipping subduction zone accommodating Africa-Iberia convergence.
- Late-metamorphic structures (assigned to D_3 and D_4 events in previous works) deforming a composite S_2 foliation in the Alpujárride Complex represent at least four different generations: two associated with steeply dipping crenulation cleavages striking broadly N–S and ENE-WSW (D_{3V}), and two subhorizontal ones generated during gravitational collapse, linked to andalusite growth (D_{3H}) and associated with brittle-ductile shear bands and detachments (D_4). These structures bear witness of dynamic interactions between tectonic stresses transmitted by Africa and the Alborán Domain and gravity.

Author statement

Alejandro Ruiz-Fuentes: conceptualization, methodology, investigation, formal analysis, writing, visualization. **Domingo Aerden**: conceptualization, methodology, writing.

Declaration of competing interest

The authors declare that they have no known competing financial interests or personal relationships that could have appeared to influence the work reported in this paper.

Data availability

Data will be made available on request.

Acknowledgements

We thank Etienne Skrzypek and two anonymous reviewers for constructive comments that helped improve an early version of the manuscript, and Toru Takeshita for his editorial work. We thank Ángel Perandrés-Villegas for making the thin sections studied for this work and Fátima Linares Ordóñez for the XCT scanning of samples. The research was carried out as part of a Ph.D. project of ARF financed by an FPU grant from the Spanish Ministery of Education and Science, Culture and Sports (FPU17/01874). Research expenses were covered by Spanish government grant CGL2016-80687-R AEI/FEDER, and Junta de Andalucía Projects P18-RT-3275 (AGORA), B-RNM-301-UGR18 (PAPEL) and RNM148. Funding for open access charge: Universidad de Granada / CBUA.

Appendix A. Supplementary data

Supplementary data to this article can be found online at https://doi.org/10.1016/j.jsg.2023.104823.

References

Abu Sharib, A.S.A.A., Sanislav, I.V., 2013. Polymetamorphism accompanied switching in horizontal shortening during isan orogeny: example from the eastern fold belt, mount isa inlier, Australia. Tectonophysics 587, 146–167. https://doi.org/10.1016/j.tecto.2012.06.051.

Acosta-Vigil, A., Rubatto, D., Bartoli, O., Cesare, B., Meli, S., Pedrera, A., Azor, A., Tajčmanová, L., 2014. Age of anatexis in the crustal footwall of the Ronda peridotites, S Spain. Lithos 210–211, 147–167. https://doi.org/10.1016/j.lithos.2014.08.018.

Aerden, D.G.A.M., 1994. Kinematics of orogenic collapse in the Variscan Pyrenees deduced from microstructures in porphyroblastic rocks from the Lys-Caillaouas massif. Tectonophysics 238, 139–160. https://doi.org/10.1016/0040-1951(94)90053-1.

Aerden, D.G.A.M., 1995. Porphyroblast non-rotation during crustal extension in the variscan lys-caillaouas massif, pyrenees. J. Struct. Geol. 17, 709–725. https://doi.org/10.1016/0191-8141(94)00090-M.

Aerden, D.G.A.M., 1998. Tectonic evolution of the Montagne Noire and a possible orogenic model for syncollisional exhumation of deep rocks, Variscan belt, France. Tectonics 17, 62–79. https://doi.org/10.1029/97TC02342.

Aerden, D.G.A.M., 2004. Correlating deformation in Variscan NW-Iberia using porphyroblasts; implications for the Ibero-Armorican Arc. J. Struct. Geol. 26, 177–196. https://doi.org/10.1016/S0191-8141(03)00070-1.

Aerden, D.G.A.M., Ruiz-Fuentes, A., 2020. X-ray computed micro-tomography of spiral garnets: a new test of how they form. J. Struct. Geol. 136, 104054 https://doi.org/10.1016/j.jsg.2020.104054.

Aerden, D.G.A.M., Sayab, M., Bouybaouene, M.L., 2010. Conjugate-shear folding: a model for the relationships between foliations, folds and shear zones. J. Struct. Geol. 32, 1030–1045. https://doi.org/10.1016/j.jsg.2010.06.010.

Aerden, D.G.A.M., Bell, T.H., Puga, E., Sayab, M., Lozano, J.A., Díaz de Federico, A., 2013. Multi-stage mountain building vs. relative plate motions in the Betic Cordillera deduced from integrated microstructural and petrological analysis of porphyroblast inclusion trails. Tectonophysics 587, 188–206. https://doi.org/10.1016/j.tecto.2012.11.025.

Aerden, D.G.A.M., Ruiz-Fuentes, A., Sayab, M., Forde, A., 2021. Kinematics of subduction in the Ibero-Armorican arc constrained by 3D microstructural analysis of garnet and pseudomorphed lawsonite porphyroblasts from Île de Groix (Variscan belt). Solid Earth 12, 971–992. https://doi.org/10.5194/se-12-971-2021.

Aerden, D.G.A.M., Farrell, T.P., Baxter, E.F., Stewart, E.M., Ruiz-Fuentes, A., Bouybaouene, M., 2022. Refined tectonic evolution of the Betic-Rif orogen through integrated 3-D microstructural analysis and Sm-Nd dating of garnet porphyroblasts. Tectonics 41, e2022TC007366. https://doi.org/10.1029/2022TC007366.

Aguado, R., Feinberg, H., Durand-Delga, M., Martín-Algarra, A., Esteras, M., Didon, J., 1990. Nuevos datos sobre la edad de las formaciones miocenas transgresivas sobre las Zonas Internas béticas: La formación de San Pedro de Alcántara (provincia de Málaga). Rev. Soc. Geol. Espana 3, 79–85.

Akkerman, J.H., Maier, G., Simon, O.J., 1980. On the geology of the Alpujarride complex in the western Sierra de las Estancias (Betic Cordilleras, SE Spain). Geol. Mijnbouw 59 (4), 363–374.

Aldaya, F., 1969. Los mantos Alpujárrides al Sur de Sierra Nevada (zona bética, provincia de Granada.). Acta Geol. Hisp. IV (5), 126–130.

Aldaya, F., García-Dueñas, V., Navarro-Vilá, F., 1979. Los Mantos Alpujárrides del tercio central de las Cordilleras Béticas. Ensayo de correlación tectónica de los Alpujárrides. Acta Geol. Hisp. 14, 154–166.

Allmendinger, R.W., Cardozo, N.C., Fisher, D., 2013. Structural Geology Algorithms: Vectors & Tensors. Cambridge University Press, Cambridge, England, p. 289.

Alonso-Chaves, F.M., Rodriguez-Vidal, J., 1998. Subsidence tectonique et sédimentation synrift associée au rifting du domaine d'Alboran au Miocène inférieur (Chaîne bétique, Espagne). Comptes Rendus Acad. Sci. - Ser. IIA Earth Planet. Sci. 326, 51–56. https://doi.org/10.1016/S1251-8050(97)83203-X.

Alonso-Chaves, F.M., Orozco, M., 2007. Evolución tectónica de las Sierras de Tejeda y Almijara: colapso extensional y exhumación de áreas metamórficas en el Dominio de Alborán (Cordilleras Béticas). Rev. Soc. Geol. Espana 20 (3–4), 211–228.

Alonso-Chaves, F.M., Orozco, M., 2012. El Complejo Alpujárride de La Axarquía: zonas de cizalla dúctiles a escala cortical y pliegues recumbentes asociados. Geogaceta 52, 5–8.

Augier, R., Agard, P., Monié, P., Jolivet, L., Robin, C., Booth-Rea, G., 2005. Exhumation, doming and slab retreat in the Betic Cordillera (SE Spain): in situ $^{40}Ar/^{39}Ar$ ages and P-T-d-t paths for the Nevado-Filabride complex. J. Metamorph. Geol. 23, 357–381. https://doi.org/10.1111/j.1525-1314.2005.00581.x.

Azañón, J.M., Goffé, B., 1997. Ferro- and magnesiocarpholite assemblages as record of high-P, low-T metamorphism in the Central Alpujarrides, Betic Cordillera (SE Spain). Eur. J. Mineral 9, 1035–1051.

Azañón, J.M., Crespo-Blanc, A., 2000. Exhumation during a continental collision inferred from the tectonometamorphic evolution of the Alpujarride Complex in the central Betics (Alboran Domain, SE Spain). Tectonics 19 (3), 549–565. https://doi.org/10.1029/2000TC900005.

Azañón, J.M., García-Dueñas, V., Martínez-Martínez, J.M., Crespo-Blanc, A., 1994. Alpujarride tectonic sheets in the central Betics and similar eastern allochthonous units (SE Spain). Comptes Rendus Acad. Sci. 318, 667–674.

Azañón, J.M., Crespo-Blanc, A., García-Dueñas, V., 1997. Continental collision, crustal thinning and nappe forming during the pre-Miocene evolution of the Alpujarride Complex (Alboran Domain, Betics). J. Struct. Geol. 19 (8), 1055–1071. https://doi.org/10.1016/S0191-8141(97)00031-X.

Azañón, J.M., García-Dueñas, V., Goffé, B., 1998. Exhumation of high-pressure metapelites and coeval crustal extension in the Alpujarride complex (Betic Cordillera). Tectonophysics 285, 231–252. https://doi.org/10.1016/S0040-1951(97)00273-4.

Balanyá, J.C., 1991. Estructura del Dominio de Alboran en la parte norte del Arco de Gibraltar. PhD Thesis. Universidad de Granada. https://digibug.ugr.es/handle/10481/50668.

Balanyá, J.C., García-Dueñas, V., 1987. Les directions structurales dans le Domaine d'Alborán de part et d'autre du Détroit de Gibraltar. Comptes Rendus Acad. Sci. 304, 929–933.

Balanyá, J.C., Azañón, J.M., Sánchez-Gómez, M., García-Dueñas, V., 1993. Pervasive ductile extensión, isothermal decompression and thinning of the Jubrique unit in the Paleogene (Alpujarride Complex, western Betics Spain). Comptes Rendus Acad. Sci. 316, 1595–1601.

Balanyá, J.C., García-Dueñas, V., Azañón, J.M., Sánchez-Gómez, M., 1997. Alternating contractional and extensional events in the alpujarride nappes of the alboran domain (Betics, Gibraltar arc). Tectonics 16, 226–238. https://doi.org/10.1029/96TC03871.

Balanyá, J.C., García-Dueñas, V., Azañón, J.M., Sánchez-Gómez, M., 1998. Reply to "comment on 'alternating contractional and extensional events in the alpujarride nappes of the alboran domain (Betics, Gibraltar arc). Tectonics 17 (6), 977–981. https://doi.org/10.1029/1998TC900006.

Balanyá, J.C., Crespo-Blanc, A., Díaz Azpiroz, M., Expósito, I., Luján, M., 2007. Structural trend line pattern and strain partitioning around the Gibraltar Arc accretionary wedge: insights as to the mode of orogenic arc building. Tectonics 26, TC2005. https://doi.org/10.1029/2005TC001932.

Bell, T.H., 1985. Deformation partitioning and porphyroblast rotation in metamorphic rocks: a radical interpretation. J. Metamorph. Geol. 3, 109–118. https://doi.org/10.1111/j.1525-1314.1985.tb00309.x.

Bell, T.H., Johnson, S.E., 1989. Porphyroblast inclusion trails: the key to orogenesis. J. Metamorph. Geol. 7, 279–310. https://doi.org/10.1111/j.1525-1314.1989.tb00598.x.

Bell, T.H., Hayward, N., 1991. Episodic metamorphic reactions during orogenesis: the control of deformation partitioning on reaction sites and reaction duration. J. Metamorph. Geol. 9, 619–640. https://doi.org/10.1111/j.1525-1314.1991.tb00552.x.

Bell, T.H., Forde, A., 1995. On the significance of foliation patterns preserved around folds by mineral overgrowth. Tectonophysics 246, 171–181. https://doi.org/10.1016/0040-1951(94)00263-9.

Bell, T.H., Welch, P.W., 2002. Prolonged Acadian orogenesis: revelations from foliation intersection axis (FIA) controlled monazite dating of foliations in porphyroblasts and matrix. Am. J. Sci. 302, 549–581. https://doi.org/10.2475/ajs.302.7.549.

Bell, T.H., Sapkota, J., 2012. Episodic gravitational collapse and migration of the mountain chain during orogenic roll-on in the Himalayas. J. Metamorph. Geol. 30, 651–666. https://doi.org/10.1111/j.1525-1314.2012.00992.x.

Bell, T.H., Fay, C., 2016. Holistic microstructural techniques reveal synchronous and alternating andalusite and staurolite growth during three tectonic events resulted from shifting partitioning of growth vs deformation. Lithos 262, 699–712. https://doi.org/10.1016/j.lithos.2016.06.031.

Bell, T.H., Rubenach, M.J., Fleming, P.D., 1986. Porphyroblast nucleation, growth and dissolution in regional metamorphic rocks as a function of deformation partitioning during foliation development. J. Metamorph. Geol. 4, 37–67. https://doi.org/10.1111/j.1525-1314.1986.tb00337.x.

Bell, T.H., Johnson, S.E., Davis, B., Forde, A., Hayward, N., Wilkins, C., 1992. Porphyroblast inclusion-trail orientation data: eppure non son girate. J. Metamorph. Geol. 10, 295–307. https://doi.org/10.1111/j.1525-1314.1992.tb00084.x.

Bell, T.H., Forde, A., Wang, J., 1995. A new indicator of movement direction during orogenesis: measurement technique and application to the Alps. Terra. Nova 7, 500–508. https://doi.org/10.1111/j.1365-3121.1995.tb00551.x.

Bell, T.H., Ham, A.P., Hickey, K.A., 2003. Early formed regional antiforms and synforms that fold younger matrix schistosities: their effect on sites of mineral growth. Tectonophysics 367, 253–278. https://doi.org/10.1016/S0040-1951(03)00126-4.

Bessière, E., Scaillet, S., Augier, R., Jolivet, L., Azañón, J.M., Booth-Rea, G., Romagny, A., Duval, F., 2022. $^{40}Ar/^{39}Ar$ age constraints on HP/LT metamorphism in extensively overprinted units: the example of the Alpujárride subduction complex (betic cordillera, Spain). Tectonics 41, e2021TC006889. https://doi.org/10.1029/2021TC006889.

Booth-Rea, G., Azañón, J.M., Goffé, B., Vidal, O., Martínez-Martínez, J.M., 2002. High-pressure, low-temperature metamorphism in alpujarride units of southeastern Betics (Spain). Compt. Rendus Geosci. 334, 857–865. https://doi.org/10.1016/S1631-0713(02)01787-X.

Booth-Rea, G., Azañón, J.M., Martínez-Martínez, J.M., Vidal, O., García-Dueñas, V., 2005. Contrasting structural and P-T evolution of tectonic units in the southeastern Betics: key for understanding the exhumation of the Alboran Domain HP/LT crustal rocks (western Mediterranean). Tectonics 24, TC2009. https://doi.org/10.1029/2004TC001640.

Bouillin, J.P., 1986. Le bassin maghrébin ; une ancienne limite entre l'Europe et l'Afrique a l'ouest des Alpes. Bull. Soc. Geol. Fr. II (4), 547–558. https://doi.org/10.2113/gssgfbull.II.4.547.

Cihan, M., Evins, P., Lisowiec, N., Blake, K., 2006. Time constraints on deformation and metamorphism from EPMA dating of monazite in the Proterozoic Robertson River Metamorphics, NE Australia. Precambrian Res. 145, 1–23. https://doi.org/10.1016/j.precamres.2005.11.009.

Comas, M.C., Delgado, F., Vera, J.A., 1979. Mapa y memoria de la Hoja nº 993 (Benalúa de Guadix). Mapa Geológico de España E. 1:50.000. In: Segunda Serie (MAGNA), Primera Edición. IGME.

Comas, M.C., García-Dueñas, V., Jurado, M.J., 1992. Neogene tectonic evolution of the Alboran Sea from MCS data. Geo Mar. Lett. 12, 157–164. https://doi.org/10.1007/BF02084927.

Crespo-Blanc, A., Orozco, M., García-Dueñas, V., 1994. Extension versus compression during the Miocene tectonic evolution of the Betic chain. Late folding of normal fault systems. Tectonics 13, 78–88. https://doi.org/10.1029/93TC02231.

Cuevas, J., 1989. Microtectónica y metamorfismo de los Mantos Alpujárrides del tercio central de las Cordilleras Béticas (entre Motril y Adra). Parte II: las Zonas Miloníticas. Bol. Geol. Min. 100 (5), 719–766.

Cuevas, J., 1991. Internal structure of the Adra nappe (alpujarride complex, Betics, Spain). Tectonophysics 200, 199–212. https://doi.org/10.1016/0040-1951(91)90015-K.

Cuevas, J., Aldaya, F., Navarro-Vilá, F., Tubía, J.M., 1986. Caractérisation de deux étapes de charriage principales dans les nappes Alpujarrides centrales (Cordillères Bétiques, Espagne). Comptes Rendus Acad. Sci. 302, 1177–1180.

Cuevas, J., Navarro-Vilá, F., Tubía, J.M., 2001. Evolución estructural poliorogénica del Complejo Maláguide (Cordilleras Béticas). Bol. Geol. Min. 11, 47–58.

DeMets, C., Iaffaldano, G., Merkouriev, S., 2015. High-resolution neogene and quaternary estimates of nubia-eurasia-north America plate motion. Geophys. J. Int. 203, 416–427. https://doi.org/10.1093/gji/ggv277.

Delgado Salazar, F., Gómez Prieto, J.A., Martín García, L., 1980. Mapa y memoria de la Hoja nº 994 (Baza). Mapa Geológico de España E. 1:50.000. In: Segunda Serie (MAGNA), Primera Edición. IGME.

Elorza, J.J., García-Dueñas, V., 1981. Mapa y memoria de la Hoja nº 1054 (Vélez-Málaga). Mapa Geológico de España E. 1:50.000. In: Segunda Serie (MAGNA), Primera Edición. IGME.

Esteban, J.J., Sánchez-Rodríguez, L., Seward, D., Cuevas, J., Tubía, J.M., 2004. The late thermal history of the Ronda area, southern Spain. Tectonophysics 389, 81–92. https://doi.org/10.1016/j.tecto.2004.07.050.

Estévez González, C., Chamón Cobos, C., 1978. Mapa y memoria de la Hoja nº 1053/1067 (Málaga/Torremolinos). Mapa Geológico de España E. 1:50.000. In: Segunda Serie (MAGNA), Primera Edición. IGME.

Farrell, T.P., 2019. Investigating the Tectonic Significance of Spiral Garnets from the Betic-Rif Arc of Southern Spain and Northern Morocco Using Sm-Nd Garnet Geochronology. M.Sc. thesis, Boston College, p. 234. https://dlib.bc.edu/islandora/object/bc-ir:108592.

Fay, C., Bell, T.H., Hobbs, B.E., 2008. Porphyroblast rotation versus nonrotation: conflict resolution. Geology 36, 307–310. https://doi.org/10.1130/G24499A.1.

Fernández-Fernández, E.M., Jabaloy-Sánchez, A., Nieto, F., González-Lodeiro, F., 2007. Structure of the Maláguide complex near vélez rubio (eastern betic cordillera, SE Spain). Tectonics 26, TC4008. https://doi.org/10.1029/2006TC002019.

Foucault, A., 1976. Complements sur la geologie de l'Ouest de la Sierra Arana et de ses environs (province de Grenade, Espagne). Bull. Soc. Geol. Fr. 18 (7), 649–658. https://doi.org/10.2113/gssgfbull.S7-XVIII.3.649.

Foucault, A., Paquet, J., 1971. Sur l'importance d'une tectogenèse hercynienne dans la région des Cordillères Bétiques (Sud de la Sierra Arana, Province de Grenade, Espagne). Comptes Rendus Acad. Sci. 272, 2756–2758.

Fyson, W.K., 1980. Fold fabrics and emplacement of an archean granitoid pluton, cleft lake, northwest territories. Can. J. Earth Sci. 17, 325–332. https://doi.org/10.1139/e80-032.

García-Dueñas, V., Navarro-Vilá, F., 1976. Alpujarrides, Malaguides et autres unités allochtones au Nord de la Sierra Nevada (Cordillères Bétiques, Andalousie). Bull. Soc. Geol. Fr. 7-XVIII-3, 641–648. https://doi.org/10.2113/gssgfbull.S7-XVIII.3.641.

García-Tortosa, F.J., López-Garrido, A.C., Sanz de Galdeano, C., 2002. Estratigrafía y estructura de la unidad de los Tres Pacos: La controversia sobre el Complejo "Almágride" en la Sierra de Almagro (Cordillera Bética, Almería, España). Rev. Soc. Geol. Espana 15, 15–25.

Geel, T., 1973. The geology of the Betic of Málaga, the Subbetic and the zone between these two units in the Vélez Rubio area (Southern, Spain). GUA Papers of Geology Ser 1 (5), 1–185.

Geel, T., Roep, T.B., 1998. Oligocene to middle Miocene basin development in the eastern betic cordilleras, SE Spain (vélez rubio corridor – espuña): reflections of west mediterranean plate-tectonic reorganizations. Basin Res. 10, 325–343. https://doi.org/10.1046/j.1365-2117.1998.00068.x.

Gómez-Pugnaire, M.T., Rubatto, D., Fernández-Soler, J.M., Jabaloy, A., López-Sánchez-Vizcaíno, V., González-Lodeiro, F., Galindo-Zaldívar, J., Padrón-Navarta, J.A., 2012. Late Variscan magmatism in the Nevado-Filábride Complex: U-Pb geochronologic evidence for the pre-Mesozoic nature of the deepest Betic complex (SE Spain). Lithos 146–147, 93–111. https://doi.org/10.1016/j.lithos.2012.03.027.

Guerrera, F., Martín-Algarra, A., Perrone, V., 1993. Late oligocene-miocene syn-/-late-orogenic successions in western and central mediterranean chains from the betic cordillera to the southern apennines. Terra. Nova 5, 525–544. https://doi.org/10.1111/j.1365-3121.1993.tb00302.x.

Guerrera, F., Martín-Martín, M., Tramontana, M., 2021. Evolutionary geological models of the central-western peri-Mediterranean chains: a review. Int. Geol. Rev. 63, 65–86. https://doi.org/10.1080/00206814.2019.1706056.

Ham, A.P., Bell, T.H., 2004. Recycling of foliations during folding. J. Struct. Geol. 26, 1989–2009. https://doi.org/10.1016/j.jsg.2004.04.003.

Hayward, N., 1990. Determination of early fold axis orientations in multiply deformed rocks using porphyroblast inclusion trails. Tectonophysics 179, 353–369. https://doi.org/10.1016/0040-1951(90)90301-N.

Hayward, N., 1992. Microstructural analysis of the classical spiral garnet porphyroblasts of south-east Vermont - evidence for non-rotation. J. Metamorph. Geol. 10 (4), 567–587. https://doi.org/10.1111/j.1525-1314.1992.tb00106.x.

Jabaloy-Sánchez, A., Fernández-Fernández, E., González-Lodeiro, F., 2007. A cross section of the eastern Betic Cordillera (SE Spain) according field data and a seismic reflection profile. Tectonophysics 433, 97–126. https://doi.org/10.1016/j.tecto.2006.11.004.

Jabaloy-Sánchez, A., Padrón-Navarta, J.A., Gómez-Pugnaire, M.T., López Sánchez-Vizcaíno, V., Garrido, C.J., 2019a. Alpine orogeny: deformation and structure in the southern iberian margin (Betics s.l.). Ch. 10. In: Quesada, C., Oliveira, J.T. (Eds.), The Geology of Iberia: A Geodynamic Approach, vol. 3. Regional Geology Reviews, pp. 453–486. https://doi.org/10.1007/978-3-030-11295-0_10. Alpine Cycle, Vergés, J., Kullber, J.C., Volume Coordinators.

Jabaloy Sánchez, A., Martín-Algarra, A., Padrón-Navarta, J.A., Martín-Martín, M., Gómez-Pugnaire, M.T., López Sánchez-Vizcaíno, V., Garrido, C.J., 2019b. Lithological successions of the internal zones and Flysch trough units of the betic chain. Ch. 8. In: Quesada, C., Oliveira, J.T. (Eds.), The Geology of Iberia: A Geodynamic Approach, vol. 3. Regional Geology Reviews, pp. 377–432. https://doi.org/10.1007/978-3-030-11295-0_8. Alpine Cycle, Vergés, J., Kullber, J.C., Volume Coordinators.

Johnson, C., Harbury, N., Hurford, A.J., 1997. The role of extension in the Miocene denudation of the nevado-filábride complex, betic cordillera (SE Spain). Tectonics 16, 189–204. https://doi.org/10.1029/96TC03289.

Johnson, S.E., 1992. Sequential porphyroblast growth during progressive deformation and low-P high-T (LPHT) metamorphism, Cooma Complex, Australia: the use of microstructural analysis to better understand deformation and metamorphic histories. Tectonophysics 214, 311–339. https://doi.org/10.1016/0040-1951(92)90204-J.

Kirchner, K.L., Behr, W.M., Loewy, S., Stockli, D.F., 2016. Early Miocene subduction in the western Mediterranean: constraints from Rb-Sr multimineral isochron geochronology. G-cubed 17, 1842–1860. https://doi.org/10.1002/2015GC006208.

Li, B., Massonne, H.J., 2018. Two tertiary metamorphic events recognized in high-pressure metapelites of the nevado-filábride complex (betic cordillera, S Spain). J. Metamorph. Geol. 36, 603–630. https://doi.org/10.1111/jmg.12312.

Lonergan, L., Platt, J.P., Gallagher, L., 1994. The internal-external zone boundary in the eastern betic cordillera, SE Spain. J. Struct. Geol. 16, 175–188. https://doi.org/10.1016/0191-8141(94)90103-1.

López Sánchez-Vizcaíno, V., Rubatto, D., Gómez-Pugnaire, M.T., Trommsdorff, V., Müntener, O., 2001. Middle Miocene high-pressure metamorphism and fast exhumation of the Nevado-Filábride Complex, SE Spain. Terra. Nova 13, 327–332. https://doi.org/10.1046/j.1365-3121.2001.00354.x.

Mares, V.M., 1998. Structural development of the soldiers cap group in the eastern fold belt of the Mt isa inlier: a succession of horizontal and vertical deformation events and large-scale shearing. Aust. J. Earth Sci. 45, 373–387. https://doi.org/10.1080/08120099808728398.

Martín-Algarra, A., 1987. Evolución geológica alpina del contacto entre las Zonas Internas y las Zonas Externas de la Cordillera Bética. PhD Thesis. Universidad de Granada, p. 1171. https://digibug.ugr.es/handle/10481/75699.

Martín-Algarra, A., Crespo-Blanc, A., Delgado, F., Estévez, A., González-Lodeiro, F., Orozco, M., Sánchez-Gómez, M., Sanz de Galdeano, C., García-Dueñas, V., 2004.

Complejo Alpujárride. Estructura. Rasgos generales. In: Vera, J.A. (Ed.), Geología de España. SGE-IGME, Madrid, pp. 416–417.
Martín-Algarra, A., Mazzoli, S., Perrone, V., Rodríguez-Cañero, R., 2009. Variscan tectonics in the malaguide complex (betic cordillera, southern Spain): stratigraphic and structural alpine versus pre-alpine constraints from the ardales area (province of Málaga). II. Structure. J. Geol. 117, 263–284. https://doi.org/10.1086/597365.
Martín-Martín, M., El Mamoune, B., Martín-Algarra, A., Martín-Pérez, J.A., 1996. The internal-external zone boundary in the eastern betic cordillera, SE Spain: discussion. J. Struct. Geol. 18, 523–524.
Martín-Rojas, I., Estévez, A., Martín-Martín, M., Delgado, F., García-Tortosa, F.J., 2007. New data from Orihuela and callosa mountains (betic internal zone, alicante, SE Spain). Implications for the "almágride complex" controversy. J. Iber. Geol. 33 (2), 311–318.
Massonne, H.J., 2014. Wealth of P-T-t information in medium-high grade metapelites: example from the Jubrique unit of the betic cordillera, S Spain. Lithos 208–209, 137–157. https://doi.org/10.1016/j.lithos.2014.08.027.
Munro, M.A., Blenkinsop, T.G., 2012. MARD-A moving average rose diagram application for the geosciences. Comput. Geosci. 49, 112–120. https://doi.org/10.1016/j.cageo.2012.07.012.
Nieto, F., Velilla, N., Peacor, D.R., Ortega Huertas, M., 1994. Regional retrograde alteration of sub-greenschist facies chlorite to smectite. Contrib. Mineral. Petrol. 115, 243–252. https://doi.org/10.1007/BF00310765.
Orozco, M., Alonso-Chaves, F.M., Nieto, F., 1998. Development of large north-facing folds and their relation to crustal extension in the Alboran domain (Alpujarras region, Betic Cordilleras, Spain). Tectonophysics 298, 271–295. https://doi.org/10.1016/S0040-1951(98)00188-7.
Orozco, M., Álvarez-Valero, A.M., Alonso-Chaves, F.M., Platt, J.P., 2004. Internal structure of a collapsed terrain the Lújar syncline and its significance for the fold- and sheet-structure of the Alborán Domain (Betic Cordilleras, Spain). Tectonophysics 385, 85–104. https://doi.org/10.1016/j.tecto.2004.04.025.
Orozco, M., Alonso-Chaves, F.M., Platt, J.P., 2017. Late extensional shear zones and associated recumbent folds in the Alpujarride subduction complex, Betic Cordillera, southern Spain. Geol. Acta 15, 51–66. https://doi.org/10.1344/GeologicaActa2017.15.1.5.
Platt, J.P., 1998. Comment on "Alternating contractional and extensional events in the Alpujarride nappes of the Alboran Domain (Betics, Gibraltar Arc)" by Juan C. Balanyá et al. Tectonics 17 (6), 973–976. https://doi.org/10.1029/1998TC900005.
Platt, J.P., Whitehouse, M.J., 1998. Early Miocene high-temperature metamorphism and rapid exhumation in the Betic Cordillera (Spain): evidence from U-Pb zircon ages. Earth Planet Sci. Lett. 171, 591–605. https://doi.org/10.1016/S0012-821X(99)00176-4.
Platt, J.P., van den Eeckhout, B., Janzen, E., Konert, G., Simon, O.J., Weijermars, R., 1983. The structure and tectonic evolution of the aguilón fold-nappe, Sierra alhamilla, betic cordillera, SE Spain. J. Struct. Geol. 5, 519–538. https://doi.org/10.1016/0191-8141(83)90057-3.
Platt, J.P., Kelley, S.P., Carter, A., Orozco, M., 2005. Timing of tectonic events in the alpujarride complex, betic cordillera, southern Spain. J. Geol. Soc. 162, 451–462. https://doi.org/10.1144/0016-764903-039.
Platt, J.P., Anczkiewicz, R., Soto, J.I., Kelley, S.P., Thirlwall, M., 2006. Early Miocene continental subduction and rapid exhumation in the western Mediterranean. Geology 34, 981–984. https://doi.org/10.1130/G22801A.1.
Porkoláb, K., Matenco, L., Hupkes, J., Willingshofer, E., Wijbrans, J., van Schrojenstein Lantman, H., van Hinsbergen, D.J.J., 2022. Tectonic evolution of the Nevado-Filábride Complex (Sierra de los Filabres, Southeastern Spain): insights from new structural and geochronological data. Tectonics 41, e2021TC006922. https://doi.org/10.1029/2021TC006922.
Puga, E., Díaz de Federico, A., 1976. Pre-Alpine Metamorphism in the Sierra Nevada Complex (Betic Cordillera Spain), 7. Cuadernos de Geología de la Universidad de Granada, pp. 161–171.
Rodríguez-Cañero, R., Jabaloy-Sánchez, A., Navas-Parejo, P., Martín-Algarra, A., 2018. Linking palaeozoic palaeogeography of the betic cordillera to the variscan iberian massif: new insight through the first conodonts of the nevado-filábride complex. Int. J. Earth Sci. 107, 1791–1806. https://doi.org/10.1007/s00531-017-1572-8.
Rodríguez-Fernández, J., 1982. El Mioceno del sector central de las Cordilleras Béticas. PhD Thesis. University of Granada, p. 224. https://digibug.ugr.es/handle/10481/32561.
Rodríguez-Fernández, J., Comas, M.C., Soria, J., Martín-Pérez, J.A., Soto, J.I., 1999. The sedimentary record of the Alboran basin: an attempt at sedimentary sequence correlation and subsidence analysis. In: Zahn, R., Comas, M.C., Klaus, A. (Eds.), Proceedings of the Ocean Drilling Program, Scientific Results, vol. 161, pp. 69–76.
Rosenbaum, G., Lister, G., Duboz, C., 2002. Relative motions of Africa, Iberia and europe during alpine orogeny. Tectonophysics 359, 117–129. https://doi.org/10.1016/S0040-1951(02)00442-0.
Rossetti, F., Faccenna, C., Crespo-Blanc, A., 2005. Structural and kinematic constraints to the exhumation of the alpujarride complex (central betic cordillera, Spain). J. Struct. Geol. 27, 199–216. https://doi.org/10.1016/j.jsg.2004.10.008.
Ruiz Cruz, M.D., Sanz de Galdeano, C., Lázaro, C., 2005. Metamorphic evolution of triassic rocks from the transition zone between the Maláguide and Alpujárride complexes (betic cordilleras, Spain). Eur. J. Mineral 17, 81–91. https://doi.org/10.1127/0935-1221/2005/0017-0081.
Ruiz-Fuentes, A., Cabrera-Porras, A., Martín-Algarra, A., 2022. Structural record of polyorogenic pre-Alpine and Alpine deformations within a major thrust nappe close to a suture zone (Internal-External Zones Boundary of the central Betic Cordillera, S Spain). Int. Geol. Rev. https://doi.org/10.1080/00206814.2022.2129472.
Sánchez-Navas, A., Oliveira-Barbosa, R.C., García-Casco, A., Martín-Algarra, A., 2012. Transformation of andalusite to kyanite in the alpujarride complex (betic cordillera, southern Spain): geologic implications. J. Geol. 120, 557–574. https://doi.org/10.1086/666944.
Sánchez-Navas, A., García-Casco, A., Martín-Algarra, A., 2014. Pre-Alpine discordant granitic dikes in the metamorphic core of the Betic Cordillera: tectonic implications. Terra. Nova 26, 477–486. https://doi.org/10.1111/ter.12123.
Sánchez-Navas, A., García-Casco, A., Mazzoli, S., Martín-Algarra, A., 2017. Polymetamorphism in the alpujarride complex, betic cordillera, south Spain. J. Geol. 125, 637–657. https://doi.org/10.1086/693862.
Sánchez-Rodriguez, L., Gebauer, D., 2000. Mesozoic formation of pyroxenites and gabbros in the Ronda area (southern Spain), followed by Early Miocene subduction metamorphism and emplacement into the middle crust: U-Pb sensitive high-resolution ion microprobe dating of zircon. Tectonophysics 316, 19–44. https://doi.org/10.1016/S0040-1951(99)00256-5.
Sanislav, I.V., 2010. Porphyroblast rotation and strain localization: debate settled!: comment. Geology 38 (4), e204. https://doi.org/10.1130/G30522C.1.
Sanislav, I.V., Bell, T.H., 2011. The inter-relationships between long-lived metamorphism, pluton emplacement and changes in the direction of bulk shortening during orogenesis. J. Metamorph. Geol. 29, 513–536. https://doi.org/10.1111/j.1525-1314.2011.00928.x.
Sanz de Galdeano, C., 1989. Estructura de las Sierras Tejeda y de Cómpeta (conjunto Alpujárride, Cordilleras Béticas), 2. Revista de la Sociedad Geológica de España, pp. 77–84.
Sanz de Galdeano, C., López-Garrido, A.C., 2003. Revisión de las unidades Alpujárrides de las sierras de Tejeda, Almijara y Guájares (sector central de la Zona Interna Bética, provincias de Granada y Málaga). Rev. Soc. Geol. Espana 16, 135–149.
Sanz de Galdeano, C., Ruiz Cruz, M.D., 2016. Late Palaeozoic to Triassic formations unconformably deposited over the Ronda peridotites (Betic Cordilleras): evidence for their Variscan time of crustal emplacement. Estud. Geol. 72 (1), e043. https://doi.org/10.3989/egeol.42046.368.
Sanz de Galdeano, C., Delgado, F., López-Garrido, A.C., 1995. Estructura del Alpujárride y del Maláguide al NW de Sierra Nevada (Cordillera Bética). Rev. Soc. Geol. Espana 8, 239–250.
Sanz de Galdeano, C., López-Garrido, A.C., García-Tortosa, F.J., Delgado, F., 1997. Nuevas observaciones en el Alpujarride del sector centro-Occidental de la Sierra de Carrascoy (Murcia). Consecuencias paleogeográficas. Estud. Geol. 53, 229–236. https://doi.org/10.3989/egeol.97535-6229.
Sayab, M., 2005. Microstructural evidence for N-S shortening in the Mount Isa Inlier (NW Queensland, Australia): the preservation of early W-E-trending foliations in porphyroblasts revealed by independent 3D measurement techniques. J. Struct. Geol. 27, 1445–1468. https://doi.org/10.1016/j.jsg.2005.01.013.
Sayab, M., Shah, S.Z., Aerden, D., 2016. Metamorphic record of the NW Himalayan orogeny between the Indian plate-Kohistan Ladakh Arc and Asia: revelations from foliation intersection axis (FIA) controlled P-T-t-d paths. Tectonophysics 671, 110–126. https://doi.org/10.1016/j.tecto.2015.12.032.
Shah, S.Z., Sayab, M., Aerden, D., Asif Khan, M., 2011. Foliation intersection axes preserved in garnet porphyroblasts from the Swat area, NW Himalaya: a record of successive crustal shortening directions between the Indian plate and Kohistan-Ladakh Island Arc. Tectonophysics 509, 14–32. https://doi.org/10.1016/j.tecto.2011.05.010.
Simancas, J.F., 2018. A reappraisal of the alpine structure of the Alpujárride complex in the betic cordillera: interplay of shortening and extension in the westernmost mediterranean. J. Struct. Geol. 115, 231–242. https://doi.org/10.1016/j.jsg.2018.08.001.
Simancas, J.F., Campos, J., 1993. Compresión NNW-SSE tardi a postmetamórfica y extensión subordinada en el Complejo Alpujárride (Dominio de Alborán, Orógeno Bético). Rev. Soc. Geol. Espana 6, 23–35.
Skrzypek, E., Schulmann, K., Stípská, P., Chopin, F., Lehmann, J., Lexa, O., Haloda, J., 2011. Tectono-metamorphic history recorded in garnet porphyroblasts: insights from thermodynamic modelling and electron backscatter diffraction análisis of inclusion trails. J. Metamorph. Geol. 29, 473–496. https://doi.org/10.1111/j.1525-1314.2010.00925.x.
Sosson, M., Morillon, A.C., Bourgois, J., Féraud, G., Poupeau, G., Saint-Marc, P., 1998. Late exhumation stages of the Alpujarride Complex (western Betic Cordilleras, Spain): new thermochronological and structural data on Los Reales and Ojen nappes. Tectonophysics 285, 253–273. https://doi.org/10.1016/S0040-1951(97)00274-6.
Stallard, A., Hickey, K., 2001. Shear zone vs folding origin for spiral inclusion trails in the Canton Schist. J. Struct. Geol. 23, 1845–1864. https://doi.org/10.1016/S0191-8141(01)00031-1.
Tubía, J.M., 1988. Estructura de los Alpujárrides occidentales: cinemática y condiciones de emplazamiento de las peridotitas de Ronda. Parte I: características litológicas. Bol. Geol. Min. 99 (II), 165–212.
Tubía, J.M., 1994. The Ronda peridotites (Los Reales nappe): an example of the relationship between lithospheric thickening by oblique tectonics and late extensional deformation within the Betic Cordillera (Spain). Tectonophysics 238, 381–398. https://doi.org/10.1016/0040-1951(94)90065-5.
Tubía, J.M., Navarro-Vilá, F., 1984. Criterios para la diferenciación entre los esquistos de grado medio del Complejo Maláguide y del Manto de Los Reales al W de Málaga. La posición del contacto de corrimiento. El borde Mediterráneo Español, Granada, pp. 33–34.
Tubía, J.M., Gil-Ibarguchi, J.I., 1991. Eclogites of the Ojén nappe: a record of subduction in the Alpujárride complex (Betic Cordilleras, southern Spain). J. Geol. Soc. 148, 801–804. https://doi.org/10.1144/gsjgs.148.5.0801.
Tubía, J.M., Cuevas, J., Navarro-Vilá, F., Álvarez, F., Aldaya, F., 1992. Tectonic evolution of the Alpujárride complex (betic cordillera, southern Spain). J. Struct. Geol. 14 (2), 193–203. https://doi.org/10.1016/0191-8141(92)90056-3.

Tubía, J.M., Navarro-Vilá, F., Cuevas, J., 1993. The Maláguide-Los Reales Nappe: an example of crustal thinning related to the emplacement of the Ronda peridotites (Betic Cordillera). Phys. Earth Planet. In. 78, 343–354. https://doi.org/10.1016/0031-9201(93)90165-6.

Vissers, R.L.M., Meijer, P.T., 2012. Iberian plate kinematics and Alpine collision in the Pyrenees. Earth Sci. Rev. 114, 61–83. https://doi.org/10.1016/j.earscirev.2012.05.001.

Williams, J.R., Platt, J.P., 2017. Superposed and refolded metamorphic isograds and superposed directions of shear during late orogenic extension in the Alborán Domain, southern Spain. Tectonics 36, 756–786. https://doi.org/10.1002/2016TC004358.

Williams, J.R., Platt, J.P., 2018. A new structural and kinematic framework for the Alborán Domain (Betic-Rif arc, western Mediterranean orogenic system). J. Geol. Soc. 175, 465–496. https://doi.org/10.1144/jgs2017-086.